Earth's Earliest Hydrosphere Recorded by the Oldest Hydrothermally-1 Altered Oceanic Crust: Triple oxygen and hydrogen isotopes in the 4.3-3.8 Ga 2 3 Nuvvuagittuq belt, Canada 4 5 Bindeman I.N.^{1*}, O'Neil J.² 6 ¹Department of Earth Sciences, University of Oregon, Eugene OR 97403, USA 7 8 ² Ottawa-Carleton Geoscience Centre, department of Earth and Environmental Sciences, 9 University of Ottawa, Canada 10 *Corresponding author bindeman@uoregon.edu 11 12 Word count: For resubmission to EPSL 13 All paper: 5750 14 Captions: 870 15 Abstract: 258 16 17 18 **Abstract** 19 The origin, evolution, and the state of Earth's hydrosphere is relevant for the timing, style and 20 intensity of plate tectonics, continental and submarine weathering, emergence of continents from 21 seawater. The temperature of the ancient oceans bears on the origin and evolution of the earliest 22 life forms. We here present a study of triple oxygen isotopes of hydrothermally altered oceanic 23 crust from the Nuvvuagittuq greenstone belt (NGB) in Canada (4.3-3.8Ga), which provides a 24 rare snapshot of the Earth's earliest hydrosphere on a planet without modern-style plate tectonics. High isotopic ($\delta^{18}O = 8-12\%$, $\Delta^{17}O = -0.02$ to -0.05%, and δD of -30-40%) values 25 26 measured in the NGB metavolcanic rocks indicate that they represent upper section of oceanic 27 crust (pillows, sediments) altered at low-temperature by seawater similar to modern submarine 28 oceanic sections, lower portion (dikes, gabbro) is not exposed. The hydrothermal process was 29 accompanied by silicification at low temperature (50-150°C) as is evidenced by elevated Δ^{17} O 30 values and triple oxygen isotope thermometry. We discuss effects of 2.7 Ga metamorphism on 31 preservation of triple oxygen isotopes and show that the hydrothermal alteration is protolithic 32 and predating metamorphism. Triple oxygen isotopes allow reconstruction of isotopic compositions of seawater and suggest that δ^{18} O of early oceans could have been comparable to 33 modern but silica-saturated. The +3% and <-5% $\delta^{18}O$ seawater would result in worse fit to the 34 35 data. The role of submarine weathering and hydrothermal silicification could have played a more 36 important role in EoArchean world with subdued role of subaerial weathering due to

insignificant continental exposure that helped balancing seawater δ^{18} O values to near modern.

38 [258 words]

39

40

41

42

43

44

45

46

47

48

49

50

51

52

53

54

55

56

57

58

59

60

61

62

63

64

65

66

67

of seawater constant.

Introduction The temperature, volume, and composition of the early hydrosphere soon after formation of the Earth bears on the evolution of the planet and life [Holland, 1984, Valley et al. 2002; Harrison, 2020]. Past efforts to better understand the composition and characteristics of the ancient hydrosphere used oxygen, silicon, and hydrogen isotopic compositions of preserved proxies such as (bio)chemical marine sedimentary archives [Knauth and Lowe, 2003; Shields and Veizer, 2002; Andrée et al. 2019; Pope et al. 2012] and hydrothermally altered-rocks [Bowers and Taylor, 1985; Muehlenbachs, 1998; Zakharov and Bindeman, 2019; Herwartz, 2021; Zakharov et al. 2021a; Johnson and Wing, 2020], with recent application of triple O isotopes [Sengupta and Pack, 2018; Bindeman, 2021; Liljestrand et al. 2020]. As oxygen is the most abundant element on and most important stable isotopic tracer on Earth, the interactions between major reservoirs of oxygen such as the lithosphere and hydrosphere, ultimately relate plate tectonics, continental weathering, and ocean temperatures s [Holland, 1984; Zakharov and Bindeman, 2019]. The temporal increase of δ^{18} O in sedimentary proxies is one of the puzzles of modern geoscience and the subject of a 50-year long and still unresolved debate [Perry, 1967; Muehlenbachs and Clayton, 1976; Knauth and Lowe, 2003; Shields and Veizer, 2002; Johnson and Wing, 2020; Bindeman, 2021]. The reliability of lower δ^{18} O values of early sedimentary archives are commonly put into question due to effects of late diagenetic/secondary alteration by subsequent low- δ^{18} O waters (Kasting et al. 2006; Liljestrand et al. 2020). However, taken together, carbonates, cherts, and shales all demonstrate a temporal increase in δ^{18} O values by 10 to 15%, unlikely to reflect the same level of secondary decrease in isotopic composition, without indicating at least in part, a true secular increasing trend of contemporaneous seawater. This trend is either reflecting that the hydrosphere became isotopically heavier while Earth's surface temperatures stayed comparable to modern [Shields and Veizer, 2002], or it alternatively is reflecting a temporal change from hotter temperatures on the early Earth, to colder conditions [Perry, 1967; Knauth and Lowe, 2003], leading to increasing isotopic fractionations $\Delta^{18}O_{proxy-water}$ (T) with decreasing temperature while keeping $\delta^{18}O$ values

One group of researchers suggest that the considerable by 10-15‰ change in $\delta^{18}O$ of seawater seems highly improbable given that $\delta^{18}O_{\text{seawater}}$ is globally balanced on timescales of 10^7 to 10^8 years by high and low-temperature planetary fluxes [Holland, 1984; Muehlenbachs, 1998; Kasting et al. 2006], such as submarine hydrothermal alteration, and surface weathering [Shields and Veizer, 2002; Muehlenbachs, 1998; Pope et al, 2012]. Supporting this hypothesis is the relatively constant $\delta^{18}O$ values recorded in ophiolites and sections of altered oceanic crust through time. These are generally interpreted to reflect relatively constant $\delta^{18}O$ isotopic compositions of seawater (Muehlenbachs and Clayton, 1976; Muehlenbachs, 1998). However, estimates of the magnitude of these fluxes, as well as their variations during different climate and supercontinent cycles, are poorly constrained and vary up to twofold, at best [e.g. Clayton and Muehlenbachs, 1976 vs. Holland, 1984]. Perhaps more importantly, the extent of coupling of isotope exchanges during water-rock interaction has only been recently studied [Kasting et al. 2006; Kanzaki, 2020a,b]. For example, an application of 2D model with decoupled water-rock interaction allows for a significantly reduced hydrothermal exchange at mid-ocean ridges [Kanzaki, 2020a,b] relaxing $\delta^{18}O$ flux constrains provided by ophiolite record.

It is particularly interesting to investigate stable isotopic compositions in the Archean and early Proterozoic during a time when the Earth's geodynamics may have differed from modern-style plate tectonics [e.g. Stern et al. 2018; Bédard, 2018]. For example, a smaller proportion of subaerially exposed crust may have been available for weathering [Bindeman et al. 2018] and submarine weathering could have played a more important role in the overall elemental and isotopic balance on the early Earth [Kasting et al. 2006; Farahat et al. 2017; Coogan and Gillis, 201]. Both low and high-T alteration is observed in the Archean oceanic crust, similar to modern [Hoffman et al. 1986] but their relative role may be different.

We here present the first stable isotopic investigation of the world's earliest exposed mafic crust from the Nuvvuagittuq greenstone belt (NGB), in the northeastern Superior Province in Canada (**Fig. 1**). Variations in ¹⁴²Nd isotopic compositions in the NGB metavolcanic rocks have been interpreted as reflective of a Hadean age of 4.3 Ga, which would make them the oldest rocks preserved on Earth [O'Neil et al. 2008; 2012]. Although its exact age is still debated (see [O'Neil et al. 2019] for review), the NGB it is at least 3.75 Ga [Cates et al. 2007], making these metavolcanic rocks contemporaneous or older than the rocks from the Isua supracrustal belt in Greenland, which have been used to constrain the composition of Earth's early oceans (Pope et

al. 2012). The NGB rocks provide a rare opportunity to investigate the seawater-rock interactions in the earliest oceanic crust and infer the composition of ancient seawater, as well as the first constraints from stable isotopes on potentially Hadean crust.

102

103

104

105

106

107

108

109

110

111

112

113

114

115

116

117

118

119

120

121

122

123

124

125

126

127

99

100

101

Geology of the Nuvvuagittuq greenstone belt

The map of the NGB is provide in Fig. 1. The dominant lithology of the NGB, called the Ujaraaluk unit, is composed of metabasaltic rocks interpreted to represent a section of early mafic crust formed in a submarine environment (e.g. [O'Neil et al. 2019]). A Hadean age for the Ujaraaluk rocks has been proposed based on the wide range of ¹⁴²Nd/¹⁴⁴Nd ratios they exhibit (O'Neil et al., 2008). Since ¹⁴²Nd is the decay product of ¹⁴⁶Sm, which has a short half-life of 103 Myrs, variations in ¹⁴²Nd/¹⁴⁴Nd can only be produced by Sm-Nd fractionation prior to 4 Ga. The correlation between ¹⁴²Nd/¹⁴⁴Nd and Sm/Nd ratios displayed by the Ujaraaluk rocks is consistent with an age of 4.3 Ga, which would make them the only known rocks formed during the Hadean (O'Neil et al., 2008; 2012). This age has however been challenged based on the oldest U-Pb zircon ages of ~3.8 Ga from rare quartz-rich zircon-bearing rocks within the NGB (Cates et al., 2013). The origin of these quartz-rich rocks and their relationship to the Ujaraaluk unit is however unclear and some authors have proposed that they only provide a minimum age for the NGB metavolcanic rocks rather than their formation age (Darling et al., 2013). Nevertheless, zircon ages from intruding felsic rocks, suggest the NGB is at least 3.75 Ga (e.g. Cates and Mojzsis, 2007). The NBG metavolcanic rocks locally preserves pillow lava structures (Fig. 2), consistent with formation on the seafloor, and the fine compositional layering observed in the Ujaraaluk unit has been interpreted to be reflective of submarine volcanic deposition (O'Neil et al., 2011). The NGB mafic metavolcanic Ujaraaluk rocks also includes laterally continuous chemogenic sedimentary rocks such as banded iron formations, cherts, and silica-rich formations (Fig. 1), typical for silica saturated seawater in the Archean (Andree et al. 2019) and early Proterozoic seafloor settings. The low Al₂O₃ and TiO₂ concentrations, as well as the seawater-like REE+Y profiles of the NGB chemical sedimentary rocks is consistent with deposition in a relatively detritus-free marine setting (Mloszewska et al., 2012).

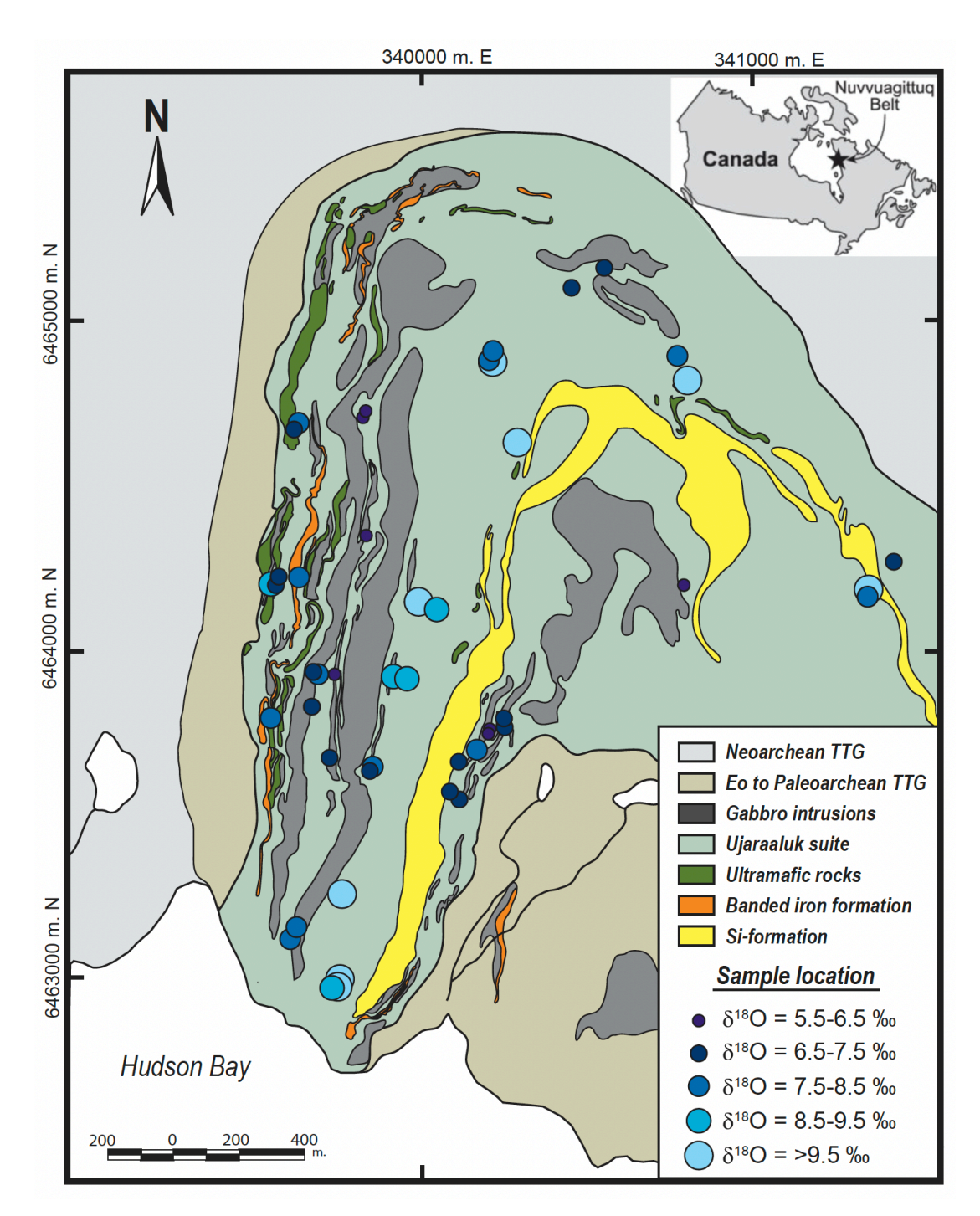


Fig. 1 Simplified geological map of the Nuvvuagittuq greenstone belt from O'Neil et al. 2011. Locations for the metabasaltic samples analyzed for this study are shown, with color and size of the symbols corresponding to measured $\delta^{18}O_{rock}$ values.



Fig. 2 Field photograph of preserved deformed pillow lavas in the Ujaraaluk unit, with differential erosion highlighting the selvages of the single pillows.

145

146

147

148

149

150

151

152

153

154

155

156

157

158

159

160

161

162

163

164

The NGB Ujaraaluk metavolcanic rocks mainly consist of cummingtonite + quartz + biotite + plagioclase ± garnet amphibolites. The unit is divided into high-Ti and low-Ti geochemical groups, the latter being further subdivided into depleted low-Ti and enriched low-Ti Ujaraaluk amphibolites, based on relative concentrations in incompatible trace elements. The three groups show distinct Al/Ti ratios, consistent with derivation from mantle sources exhibiting variable degrees of depletion (O'Neil et al. 2011). The Ujaraaluk geochemical groups also follow a chemostratigraphy in the NGB, reminiscent of subduction initiation settings [Turner et al., 2014; O'Neil et al., 2019]. The base of the volcanic sequence is composed of the high-Ti Ujaraaluk rocks that follow a tholeitic differentiation trend. The high-Ti Ujaraaluk rocks are superimposed by the chemical sedimentary rocks, followed by the depleted low-Ti Ujaraaluk rocks with boninitic geochemical affinities, and the enriched low-Ti Ujaraaluk at the top of the sequence, which compositionally resembles calc-alkaline lavas (O'Neil et al. 2011). The Ujaraaluk unit locally comprises a cordierite-anthopyllite assemblage, which exhibits low Ca and high Mg contents, interpreted to reflect hydrothermal alteration of mafic crust, similar to what is observed in volcanogenic massive sulfide deposit environments, consistent with a seafloor setting (O'Neil et al., 2019). The NGB includes ultramafic rocks occurring as discontinuous body, mainly composed of serpentine + talc + tremolite + hornblende + chromite. Their whole-rock composition is mainly controlled by olivine fractionation and interpreted to be cogenetic ultramafic cumulates that fractionated from the mafic Ujaraaluk liquids (O'Neil et al. 2007; 2019). The NGB ultramafic rocks are divided into the same geochemical groups as the Ujaraaluk mafic suite, displaying the same distinct Al/Ti ratios and following the same chemostratigraphy within the NGB. The metavolcanic rocks are intruded by a series of gabbroic sills (Fig. 1) interpreted to have been emplaced at different times in the NGB. Large >100 m. wide sills that can be continuously traced over 2 km along strike display gneissic textures and yielded a ~4.1 Ga Sm-Nd isochron age (O'Neil et al., 2012), while smaller coarse-grained gabboic bodies are interpreted to have intruded the NGB at ~2.7 Ga (David et al., 2009) and represent the youngest known magmatic episode in NGB. Garnet Sm-Nd ages from the NGB suggest it was metamorphosed at ~2.7 Ga (O'Neil et al., 2012) up to amphibolite facies (O'Neil et al., 2007; Cates et al., 2009), likely during the Neoarchean regional metamorphism of the northeastern Superior Province (e.g. Percical et al., 2012). Despite evidence that some elements may have been mobilized during post-magmatic processes, the whole-rock composition of the Ujaraaluk unit appears to have not been significantly affected by metamorphism (O'Neil et al., 2011). For example, a number of Ujaraaluk rocks display low CaO contents inconsistent with a primary igneous composition, but have been interpreted to reflect alteration of the igneous protolith of these rocks prior to metamorphism (O'Neil et al., 2011). Furthermore, the Earth's earliest fossilized microorganisms have been described in least metamorphosed sedimentary jaspers [Dodd et al. 2017] within the NGB suite, as well as the original organic graphite, although the latter is controversial [Papineau et al. 2011].

Methods

Analytical methods. We here report isotopic analyses on all major rock types of the NGB, including samples from the Ujaraaluk unit, the ultramafic rocks, the chemical sedimentary rocks, the gabbroic intrusions and the surrounding felsic plutonic rocks. Data is presented in **Table 1**. All stable isotope analyses were performed at the University of Oregon Stable Isotope Lab, whole-rock chemical data are from O'Neil et al. [2011; 2019]. Oxygen isotope measurements for δ^{18} O relied on 1 to 1.5 mg of material, predominantly single chunks of amphibole and were performed by laser fluorination and gas-source mass spectrometry (MAT253). We used purified BrF₅ as a reagent and Hg diffusion pump to clean the excess of F₂ gas, then converted purified O₂ into CO₂ and analyzed it in a dual inlet mode on the MAT253 mass spectrometer, integrated with the vacuum line, as this method is most precise for δ^{18} O determination (e.g. [Bindeman, 2008]). Samples yields were measured in a calibrated volume using a Baratron gauge. San Carlos

Olivine ($\delta^{18}\text{O}=5.25\%$, UWG2 garnet, 5.80% [Valley et al. 1995] and an in-door UOG garnet standard calibrated relative to the other two ($\delta^{18}\text{O}=6.52\%$) were used to calibrate the data on VSMOW scale. Each session included analyses of 4 to 6 standards, and correction for day-to-day variability was 0 to 0.2%. Standard CO₂ gas was used as a working standard and periodically rerun against OZTECH CO₂ gas. Errors for standards in individual sessions ranged from ± 0 to $\pm 0.11\%$ and on average was better than $\pm 0.08\%$. Samples from sessions with low yields were rerun using an airlock sample chamber. Yields were in the 11-16 μ mols/mg range and demonstrated no correlation with δ^{18} O. Coexisting garnets were also analyzed in six samples and yielded values comparable to amphiboles or whole-rock samples. Garnet has Δ^{18} Ogarnet-whole rock =0 $\pm 0.5\%$ fractionation for metabasaltic compositions (e.g. Bindeman and Serebryakov, 2011).

For triple oxygen isotope analyses generated gas was run as O_2 in sessions with SCO standard ($\Delta'^{17}O = -0.052\%$, [Miller et al. 2020] and utilized a triple O continuous flow line constructed for precise triple O isotopes measurements [Bindeman et al. 2018]. The generated O_2 gas was put through a 8 ft long gas chromatographic column at room temperature for its purification from NF_x compounds. Generated gases were additionally frozen on a 5A zeolite and then released into the bellow of the mass spectrometer by LN2-ethanol mix over 10 min. GC and zeolite traps were degassed with flowing He at 200°C for 15-20 min between each sample. The purified O_2 gas was run 4-10 times for 8 cycles in a dual inlet mode, against a oxygen standard gas well calibrated relative to VSMOW at the University of Washington on a MAT253 isotope ratio mass spectrometer. Precision of $\Delta'^{17}O$ is around $\pm 0.01\%$ (Table 2).

Hydrogen isotopes and water concentrations were measured using a high temperature conversion elemental analyzer (TC/EA with glassy carbon) held at 1450°C and integrated with the same MAT 253 mass spectrometer. Biotite, cummingtonite, hornblende and whole-rock samples dominated by anthophyllite, were wrapped up in Ag foil using the 53-150 μm size fraction. 1 to 4 mg of samples were precisely weighed using a Costech 6-digit balance were degassed at 130°C in a vacuum overnight oven prior to loading into TCEA carousel to remove any absorbed water. Analyses of the unknowns were interspersed with solid standards.

Standards were USGS57 (biotite) and USGS58 (muscovite; Qi et al., 2017) and water (VSMOW, Lake Louise) welded in Ag caps (Qi et al., 2010). During analysis, released water is instantaneously converted to H₂ and CO gas by a pyrolysis reaction with the glassy carbon, and reaction products were passed through a gas chromatographic column using He as a carrier gas,

followed by CONFLOW open split, then analysis on MAT253 against the reference gas of known composition. Each session was calibrated by H3 factor determined in the beginning of each session. Hydrogen isotopes and total H₂O were determined from the yields of H₂ by comparison to standards of known weight. Precision of H₂O content is ±0.02-0.04 wt% and within 1-3‰ for δD.

232233

234

235

236

- Isotopic notations and fractionation equations. In addition to conventionally defined $\delta^{18}O$ and $\delta^{17}O$ values as (R_{sample}/R_{VSMOW} -1)•1000 where R is $^{18}O/^{16}O$ and $^{17}O/^{16}O$ ratios in samples and VSMOW water standard [Sharp, 2017], we used primed notations of $\delta^{\prime 18}O$ and $\delta^{\prime 17}O$.
- 237 Primed, or linearized δ values are expressed as [Miller et al. 2020]:

238
$$\delta^{18,17}O = 1000\ln(\delta^{18,17}O/1000+1)$$
 [1]

- They are not significantly different numerically from conventionally defined δ 's (typically by
- 240 0.0X‰), but the transformation using the logarithmic scale allows for simple algebra when
- relating isotope fractionations $1000 \ln \alpha^{18}$ and $\Delta^{'18}$ O values. In primed coordinates:

242
$$\Delta'^{18}O_{proxy-water}(T) = \delta'^{18}O_{proxy} - \delta'^{18}O_{sw}$$
 [2]

Similar equation holds for ¹⁷O. Equation [2] relates measured and linearized δ'¹⁸O and δ'¹⁷O values with temperature-dependent fractionation factors.

$$1000 \ln \alpha^{18}_{\text{proxy-water}}(T) = \Delta^{18}_{\text{oproxy-water}}(T)$$
 [3]

246

Estimation the $\delta^{'18}O_{sw}$ value of seawater based on the $\delta^{'18}O$ value of the solid proxy that interacted with it and reached equilibrium is:

$$\delta^{18}O_{sw} = \delta^{18}O_{proxy} - \Delta^{18}O_{proxy-water} (T)$$
 [4]

250

The linearized notations allow the $\Delta^{17}O$ (triple O) to be expressed as:

252
$$\Delta^{17}O = \delta^{17}O - 0.528 \cdot \delta^{18}O$$
 [5]

- 254 which measures deviation from a mass dependent fractionation line with a reference slope. Many
- 255 terrestrial processes occurring at low and medium temperatures follow a slope of 0.528
- 256 (Schauble and Young, 2021), which we adopted here. The highest temperature natural processes

follow a slope of 0.5305, which used in many other publications. Isotopic fractionations of ^{17}O as a function of temperature is recast using $\Delta'^{17}O$ of water and solid proxy as:

$$\Delta \Delta'^{17}O_{\text{proxy-water}}(T) = \Delta'^{17}O_{\text{proxy}} - \Delta'^{17}O_{\text{water}}$$
 [6]

This paper builds upon the recent application of $\delta^{17}O$ alongside $\delta^{18}O$. The $\Delta'^{17}O$ and $\delta'^{17}O$ values have their own independent fractionation equations [Sharp et al. 2016; Sengupta and Pack, 2018; Bindeman, 2021], potentially allowing for independent resolution of the effects of temperature and isotopic values of the ancient seawater, which is the main goal of this study. For quartz, we used $\Delta'^{18}O_{quartz-water}$ (T) and $\Delta\Delta'^{17}O_{quartz-water}$ (T) fractionation equations from Sharp et al. (2016). For basalt-water we used $\Delta'^{18}O_{basalt-water}$ (T) fractionation equation from Zhao and Zheng (2003), but for the $\Delta\Delta'^{17}O_{basalt-water}$ (T) we used the following semi-empirical equation:

269
$$\Delta \Delta^{17}O_{\text{basalt-water}} = -6 \cdot 10^6 \text{ x}^3 + 17138 \text{ x}^2 - 11.88 \text{ x}$$
 [7]

where x is 1/T, K^{-1} . When $\Delta'^{17}O$ is plotted vs. $\delta'^{18}O$ for basalt, the curve is comparable in shape to quartz, but shorter long the $\delta'^{18}O$ axis because basalt-water fractionation is smaller by $\sim 15\%$ compared to quartz-water. The $\Delta'^{17}O$ is shifted down relative to the quartz-water fractionation curve, as measured and computed for Fe-Mg-rich minerals and micas (Bindeman et al. 2018; Schauble and Young, 2021).

Results

Stable isotopes and compositional trends

Sample description and obtained stable isotopic values are presented in **Table 1**; $\delta^{18}O$ values for the metavolcanic samples are plotted on Fig. 1. The main result of the present study is the discovery of high $\delta^{18}O$ (8-16‰), $\Delta'^{17}O$ (-0.02 to -0.05‰) and δD (-30-40‰) values in most samples from the Ujaraaluk metavolcanic rocks (**Fig. 3**; **Table 1**). A combination of $\delta^{18}O$ and recently developed novel $\Delta'^{17}O$ parameter (**Fig. 4-5**) allows us to resolve a range of temperatures of interaction as well as to estimate the isotopic compositions of the fluids involved. The measured $\delta^{18}O$ values in metabasalts range between 6 to 12‰ and are higher than the mantle value. This range of $\delta^{18}O$ values is typical of low-temperature (~<150°C) alteration products observed in the shallow portion of modern oceanic crust (pillow lavas and sediments) obtained

from drillcores, as well as exposed modern seafloor sections or exposed Phanerozoic settings [Alt and Teagle, 2000; Bowers and Taylor, 1985; Alt, 2012; Caro et al. 2017]. No difference is observed between the Ujaraaluk rocks at the base or at the top of the volcanosedimentary succession, while higher δ^{18} O values of up to +16‰ are found in the chemical sedimentary rocks, stratigraphically between the high and low-Ti Ujaraaluk rocks. Despite regional sampling of the NGB, we do not observe an equivalent of the low- δ^{18} O zone, indicative of the higher temperature alteration that commonly characterizes the lower part of Phanerozoic and older ophiolites [Alt and Teagle, 2000; Gregory and Taylor, 1981; Zakharov and Bindeman, 2019], consistent with the absence of sheeted dikes at NGB. The lower δ^{18} O values measured in the ultramafic cumulates (5.6 to 6.6‰), are similar to the isotopic compositions of modern MORB and boninite glasses [Eiler, 2001; Coulthard et al. 2020; Miller et al. 2020]. Additionally, the 2.7 Ga gabbroic sills intruding the NGB display mantle-like δ^{18} O values around 5.7‰ (**Table 1, Fig. 3**). This signifies that the Neoarchean metamorphism did not result in redistribution of oxygen and implies that NGB rocks preserve protolithic high δ^{18} O values, predating the regional metamorphism.

We observe no spatial relationship in the field or difference in $\delta^{18}O$ values between the different geochemical groups of Ujaraaluk rocks (**Fig. 1-3b-4, S1-S2**). Since the distinct Al₂O₃/TiO₂ ratios of the Ujaraaluk geochemical groups is believed to reflect variable degrees of depletion of their source, this suggests that the stable isotopic ranges are not inherited from the mantle source, but rather the result of post-emplacement hydrothermal alteration that affected all NGB geochemical groups without preference.

Compositional trends, temperature of water-rock interaction

The NGB rocks display a strong correlation between $\delta^{18}O_{rock}$ and silica content (**Fig. 4**) and more scattered negative correlations with MgO and FeO concentrations (**Fig. S1**). The most straightforward explanation of the silica- $\delta^{18}O_{rock}$ correlation is simple addition of silica to variously hydrothermally altered rocks at 100-200°C, as is illustrated on **Fig. 4-5**. However, the whole range of alteration cannot solely be explained by mechanical addition of silica.

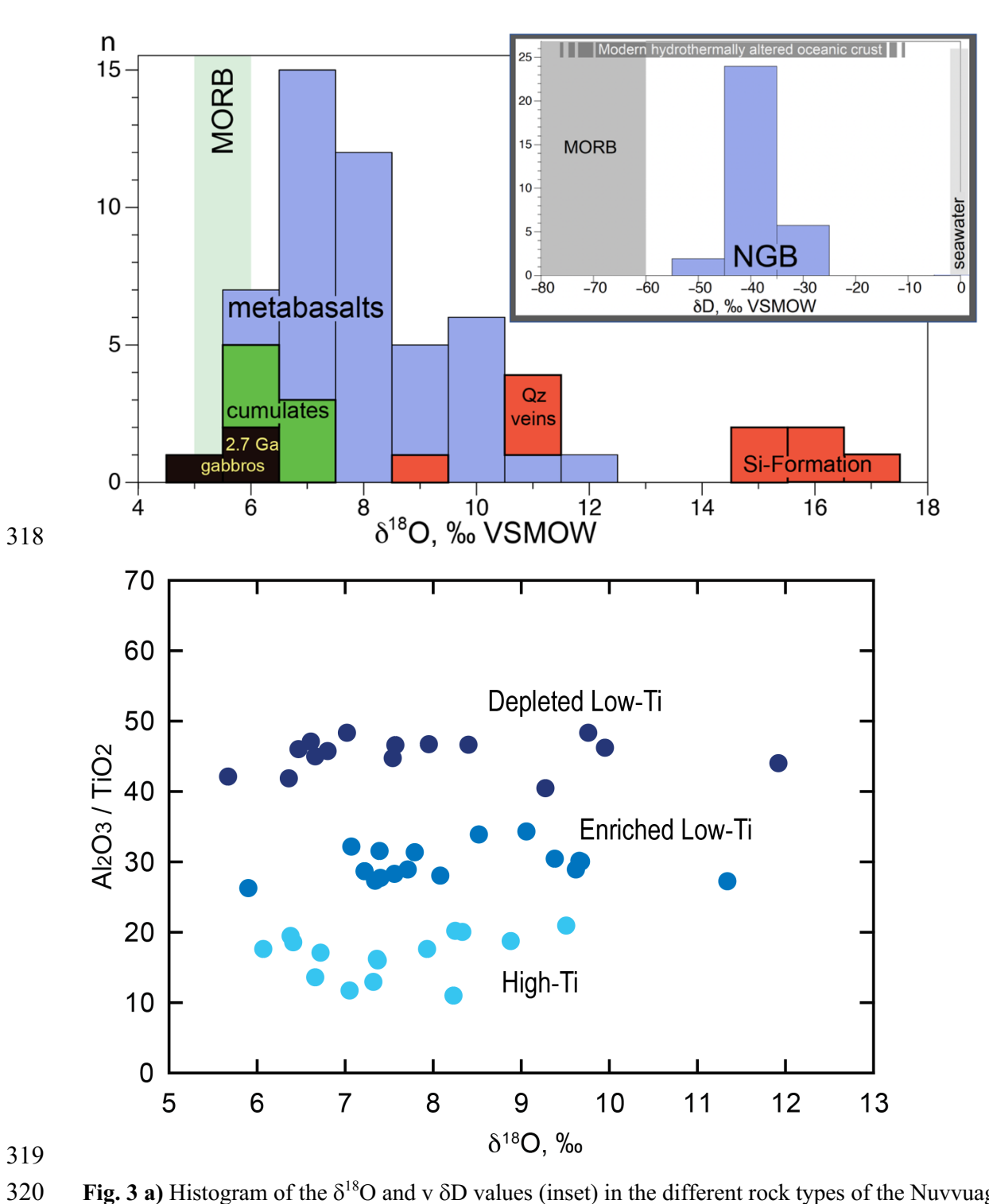
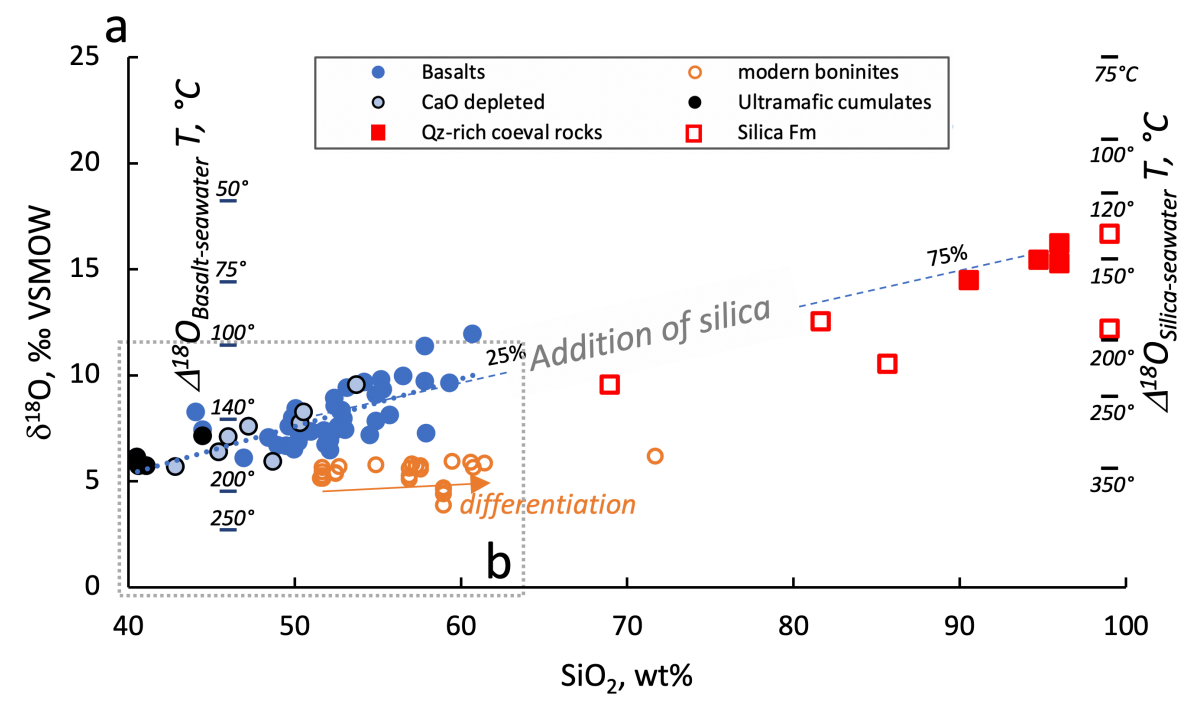
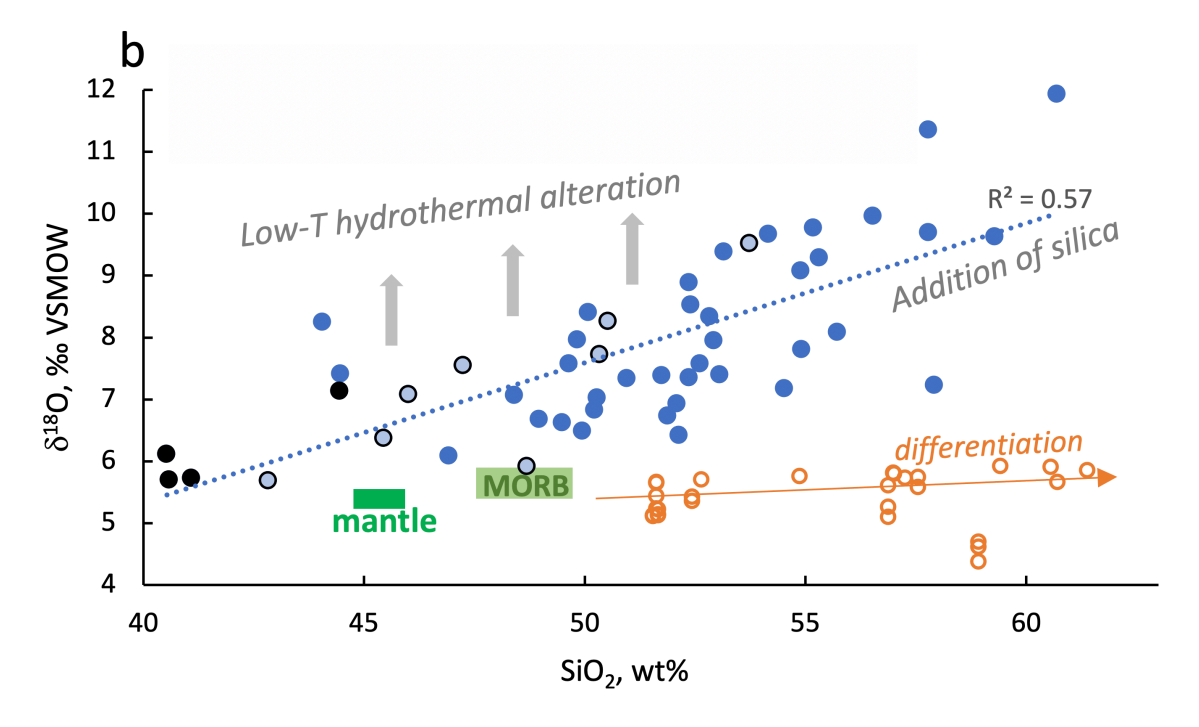


Fig. 3 a) Histogram of the $\delta^{18}O$ and v δD values (inset) in the different rock types of the Nuvvuagittuq greenstone belt and b) Al_2O_3/TiO_2 ratios vs. $\delta^{18}O$ values for different compositional groups of Ujaraaluk metabasalts. Data are presented in Table 1. MORB $\delta^{18}O$ and v δD values are from Gregory and Taylor (1981) and Dixon et al. (2017).

Fig. 4 δ^{18} O vs SiO₂ diagrams for the NGB Ujalaaluk rocks (blue symbols), a) full SiO₂ range of all analyzed lithologies, b) zoomed in range (see Table 1 for data) focusing on the Ujaraaluk samples. Modern boninite suite from [Coulthard et al. 2020] is shown for comparison, as some NGB rocks are analogous to boninites [O'Neil et al., 2011; Turner et al. 2014]. Igneous differentiation of MORB basalts would result in negligible increase of δ^{18} O values (by 0.1-0.2%; [Eiler, 2001]) as is also exemplified by the boninite suite. Low temperature (<150°C) alteration can account for the range and increase in δ^{18} O values observed in the NGB rocks, while addition of chemogenically-precipitated SiO₂ can also explain the positive correlation with SiO₂. Ca-depleted are cordierite-anthophyllite rocks, are interpreted to have lost most Ca due to hydrothermal alteration [O'Neil et al., 2019].





For example, rocks with SiO₂ content as low as 44 wt%, unlikely to have been affected by silica addition, extend to $\delta^{18}O_{rock}$ values up to 8% (Fig. 4). Likewise, at any given SiO₂ content, variation in $\delta^{18}O$ values of 3-5%, suggesting a shift in oxygen isotope compositions without silica addition. There is no trend of increasing $-\delta^{18}O_{rock}$ when approaching chemogenic silica formation (Fig. 1, S2).

Isotopic fractionations ($\Delta^{18}O = \delta^{18}O_{\text{rock}} - \delta^{18}O_{\text{sw}}$) greater than ~6-7% between 0% modern seawater (or -0.75% pre-glacial seawater) and 5.7% mantle-derived basalts persist at temperatures lower than ~200°C, but in order to generate $\delta^{18}O_{rock}$ of 12%, temperatures no higher than $\sim 90^{\circ}$ C are required [Zhao and Zheng, 2003]. The high $\delta^{18}O_{rock}$ values measured in the NGB submarine rocks thus resulted from low-temperature hydrothermal alteration. The $\delta^{18}O_{rock}$ values of 8.5% measured in rocks that have not undergone silica addition (samples with <45 wt% SiO₂), would permit higher hydrothermal interaction temperatures of up to 140°C. The addition of hydrothermal silica with relatively high δ^{18} O values to rocks showing minimal hydrothermal alteration may represent another endmember process that contributed to the overall range of δ^{18} O values measured in the NGB rocks. As silica shows the largest isotopic fractionation with water in nature, its low temperature precipitation yields the highest δ^{18} O values measured in terrestrial rocks [e.g., Eiler, 2001; Sharp et al. 2016]. This process would require temperatures of 150°C or less (Fig. 4). Therefore, in order to account for the range of δ¹⁸O values up to 12‰ of the NGB rocks and the strong correlation with SiO₂, two related processes must operate together: 1) typical low-temperature alteration of basaltic crust, which may include formation of clays and carbonates as alteration products [Alt and Teagle, 2000; Alt, 2003] and 2) direct addition of hydrothermal silica precipitated from seawater.

358359

360

361

362

363

364

365

366

337

338

339

340

341

342

343

344

345

346

347

348

349

350

351

352

353

354

355

356

357

Triple Oxygen isotopes

To further illustrate and resolve the effects of hydrothermal alteration and addition of silica, we investigated triple oxygen isotope of the metavolvanic rocks and their garnet separates, as well as coeval sedimentary silica, covering the full range of $\delta^{18}O$ and SiO_2 spectra. Furthermore, consideration of $\Delta^{\prime 17}O$ allows to obtain better temperature estimations, and to separate the effects of silica addition from low-temperature hydrothermal alteration (**Fig. 5**). If the addition of silica is taken as the predominant mechanism affecting the $\delta^{18}O$ and $\Delta^{\prime 17}O$ values

of the rocks, water-rock interaction temperatures would be between 125°C and 225°C. Overall, **Fig. 5** shows that the entire NGB rock suite can be explained by a mixture between the alteration products with chemical sediments and unaltered mantle-derived basalts (yellow triangular field in **Fig. 5**). The data is consistent with low to medium-temperature hydrothermal alteration environments, similar to modern-day pillow sections (**Fig. 2**) of submarine oceanic crust covered by chemogenic oceanic sediments.

 It is also noticeable that the data plot in proximity to computed modern seawater-oceanic crust alteration curves (**Fig. 5**), suggesting that the results can be explained by the involvement of seawater comparable in $\delta^{18}O$ and $\Delta'^{17}O$ to modern. Seawater with a lower $\delta^{18}O$ value of -5‰ (also computed here to account for higher $\Delta'^{17}O$, as required for global mass balance of triple O isotopes [Sengupta and Pack, 2018; Bindeman, 2021]), would result in lower temperature of interaction and a worse overall fit of the data points (**Fig. 6**). $\delta^{18}O$ values lower than -10‰ for seawater, often suggested for Precambrian seawater, based on sedimentary archives [Knauth and Lowe, 2003; Shields et al., 2002], would result in improbable solutions in the case of the studied NGB rocks.

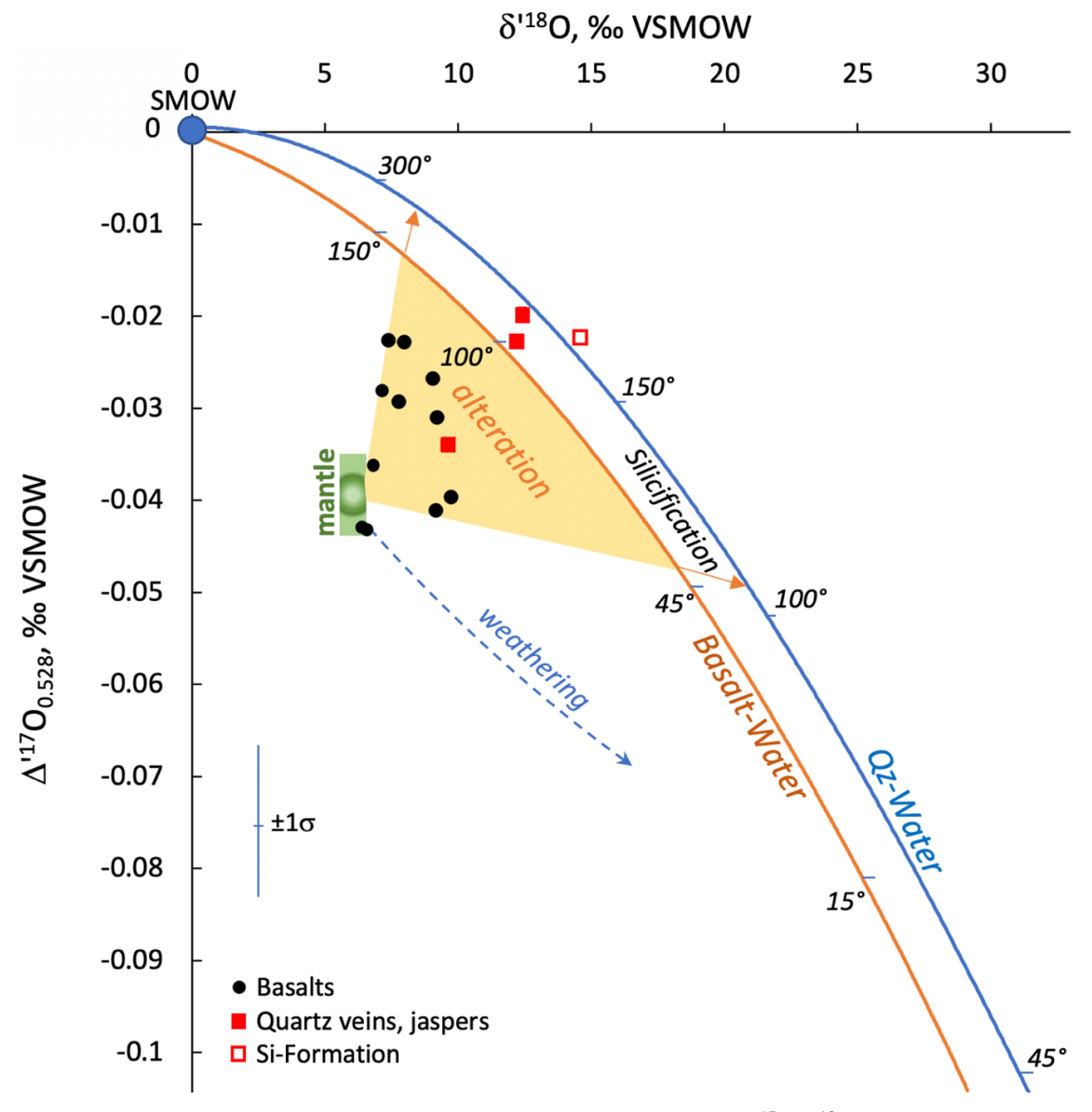


Fig. 5 Triple oxygen isotopes for the studied rocks compared to the $\Delta^{117}\text{O-}\delta^{18}\text{O}$ Qz-water fractionation curve [from Sharp et al., 2016] emanating from the modern ocean water, and basalt-seawater lines, computed in this work. Notice that the NGB rocks plot between mixing lines connecting mantle-derived rocks and seawater-equilibrated hydrothermally-altered component(s) at temperature of alteration between >45°C and <150°C (yellow triangular field). Seafloor and subaerial weathering occurring at low temperature would lead to much lower $\Delta^{117}\text{O}$ values and is not supported by the data. Concurrent silicification trends produced by silica precipitated from seawater are shown by orange arrows extending

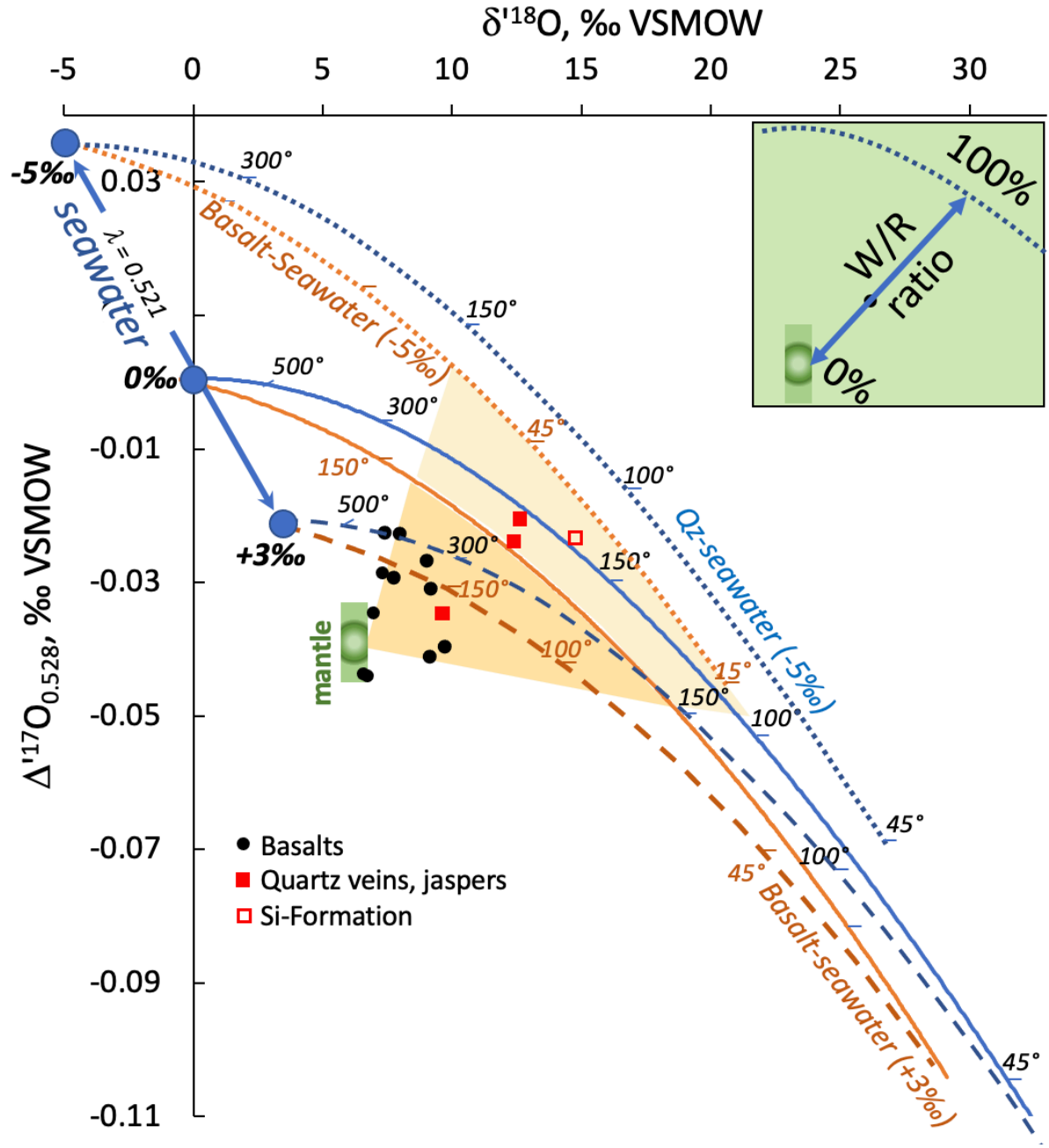


Fig. 6. Triple oxygen isotopic data (same data as in Fig. 5) but assuming different $\delta^{18}O$ values of seawater, ranging from -5 to +3‰. Change in $\delta^{18}O$ is accompanied by a change in $\Delta^{'17}O$ along a blue line with a slope of 0.521 [Bindeman, 2021]. Assuming a water value of -5‰ would result in ~20° to 150°C temperature of water-rock interaction and silicification, as well as lower water/rock ratios (illustrated on green inset). Assuming seawater with a $\delta^{18}O$ value of +3‰ would result in higher temperatures of interaction (~80° to 400°C) and greater water-rock ratios for basalt-water interaction; in addition, quartz samples would plot outside of realistic quartz-water equilibration curves.

Hydrogen isotopes

Hydrogen isotopic variations were measured in whole-rock Ujaraaluk samples (water is predominantly concentrated in the hydrated minerals cummingtonite, hornblende, and anthophyllite (e.g. O'Neil et al. 2011), and chloritzed biotite. Hydrogen isotopic analyses yielded a surprisingly uniform and high range of δD values, from -35 to -42‰ (**Fig. 7**). In a modern geological setting, δD values around -30‰ are characteristic of the higher isotopic end of submarine hydrothermal greenschist alteration products (-20 to -50‰, Bowers and Taylor, 1985; Alt and Teagle, 2000; Zakharov and Bindeman, 2019; Stakes and O'Neil, 1982). The temperatures for the alteration of the NGB metavolcanic rocks' protolith, derived from the δD-δ¹⁸O systematics (**Fig. 7b**), is consistent with 100-200°C similar to the temperature range obtained from triple oxygen isotopes. While the preservation of relatively elevated δD values measured in the NGB rocks metamorphosed to amphibolite facies should be taken with caution, the hydrogen isotopic compositions seem to broadly support the main result obtained from the major element oxygen, indicative of seafloor alteration processes. Secondary isotopic alteration, weathering effects and δD-δ¹⁸O correlations would all result in lower δD values, further

Silicification Trends

discussed in the **Fig.** 7 and in the Supplementary information.

In order to assess the possibility of silicification of basaltic rocks similar to the NGB rocks, we have performed flush calculations when a seawater composition is equilibrated with rocks at progressively greater water/rock ratios, using a hydrothermal program CHIM-XPT (Reed et al. 2010). We used silica-saturated seawater as an input parameter because silica was likely saturated in the Archean seawater prior to the advent of silica secreting organisms such as diatoms [Andrée et al. 2019]. Runs from 25°C to 200°C were performed and included both equilibrium calculation of seawater-basalt reaction at different water/rock ratios (**Fig. 8**), and flush calculations in which dissolved amorphous silica was allowed to precipitate in pore space at hydrothermal process thus increasing bulk rock SiO₂.

Equilibrium calculations resulted in a minor SiO_2 gain, changing SiO_2 composition of whole-rock by ~ 1 wt%, but leaching Ca, as expected for hydrothermal processes (**Fig. 8**). The flush calculations with precipitation of silica in the porespace result in quantitatively significant gain of SiO_2 , which fills available porosity in a rock at hydrothermal conditions. The amount of

precipitated silica is linearly proportional to water fluxed through the rocks, as well as the amount of primary and secondary porosity, and water/rock ratio of 100 is sufficient to explain observed silica gain. It is thus the second mechanism that is likely responsible for most silicification processes observed in NGB rocks (**Fig. 3**), explaining their high δ^{18} O values.

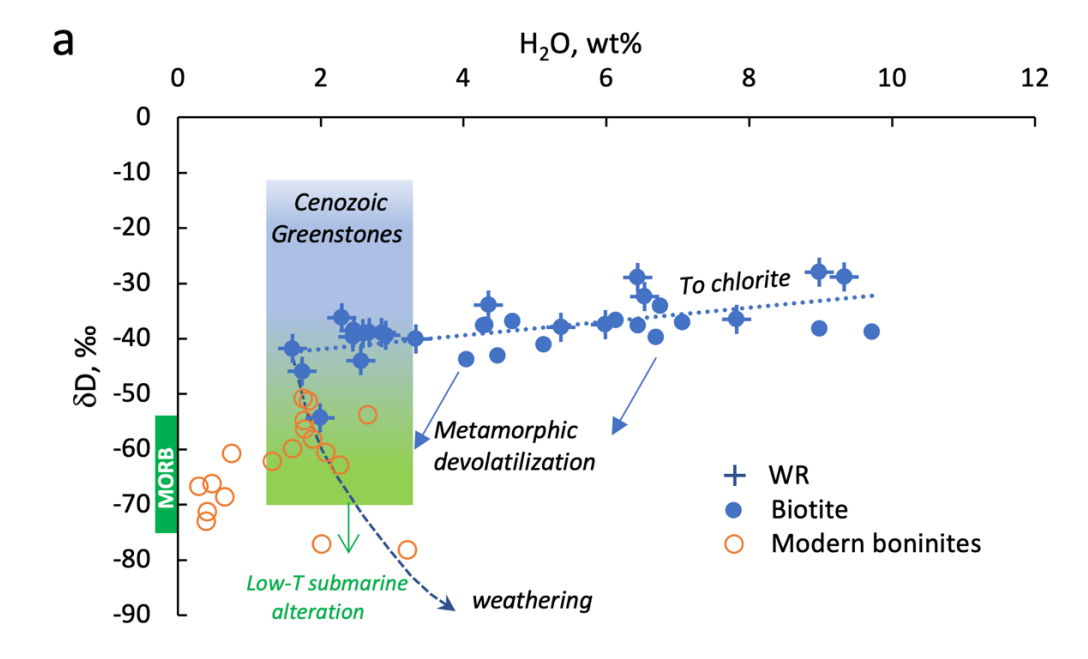
As hydrogen and oxygen isotopes typically change ahead of chemical and mineralogical change during water-rock interaction, hydrothermal alteration with indicated amount of silicification would achieve equilibrium with percolating hydrothermal fluid. Considering that percolation of fluids is channelized (e.g. dual-porosity model, DePaolo et al. 2006) high amplitude variations of water-rock ratio is expected. In other words strongly altered and equilibrated areas fluxed by large amount of fluid will be next to minimally affected areas, explaining range in δ^{18} O values.

Discussion

The NGB represents a rare remnant of early oceanic crust and offers a unique window into Earth's earliest environments. We note that the least altered NGB rocks exhibit stable isotopic compositions comparable to the modern mantle implying that the upper portion of the Earth's lithosphere may have preserved its δ^{18} O, Δ'^{17} O and δ D compositions at least since 3.8 Ga and perhaps 4.3 Ga. Because the NGB experienced a protracted thermal history after hydrothermal alteration, high-grade metamorphism at 2.7 Ga, it is crucial to examine if/how these post-magmatic processes may have affected the stable isotopes, to establish if they reflect protolithic compositions. Previous work on hydrothermally altered rocks metamorphosed to amphibolite facies from Karelia [Bindeman and Serebryakov, 2011], demonstrated conservation of the world's lowest δ^{18} O, (-27.5‰) protolithic values, including the preservation of steep δ^{18} O gradients. These values and gradients were initially generated by water-rock interaction at variable water-rock ratios by ultra-low- δ^{18} O glacial meltwater during the 2.4 and 2.3 Ga Snowball Earth events.

Likewise, δ^{18} O values of -11‰ in ultrahigh pressure metamorphic coesite-bearing rocks from Dabie Shan in China [Rumble and Yui, 1998, and hundred subsequent papers] are interpreted as protolithic compositions, reflecting pre-metamorphic interaction with surface-derived glacial meltwaters. As oxygen is a major element in silicate Earth, metamorphic recrystallization of the NGB rocks' primary crystalline assemblages likely resulted in only







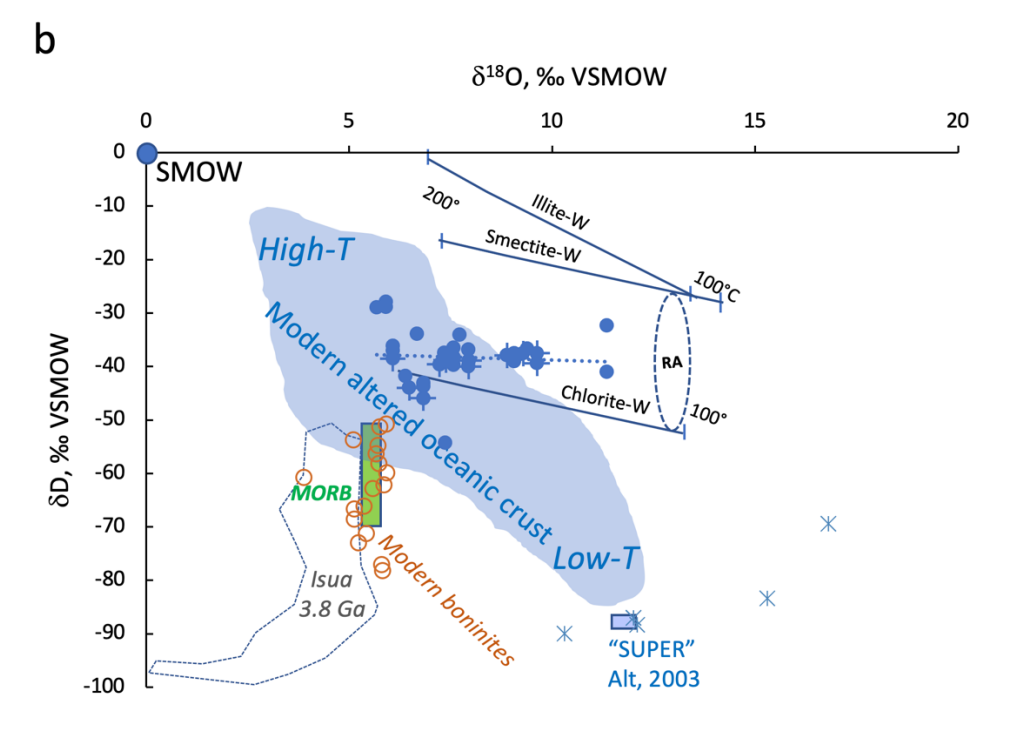


Fig. 7 Hydrogen- H_2O and $\delta^{18}O$ correlation for NGB rock suite.

a) δD – H₂O diagram comparing the NGB rocks and modern (Cenozoic) hydrothermally altered seafloor products [Bowers and Taylor, 1985; Alt, 2003; Stakes and O'Neil, 1982; Alt and Teagle, 2003]. δD values of mantle and modern boninites are shown for comparison. Various isotopic shift trends from known processes are represented with arrows [Valley, 1986; Bindeman and Serebryakov, 2010]. Notice that an increase in water content in the NGB rocks is not accompanied by a decrease in δD, suggesting that it was caused by a fluid comparable to seawater during hydrothermal or metamorphic processes.

There is no difference in δD values between coexisting anthophyllite, biotite and whole-rock, within the same rock samples (Table 1).

b) δD vs $\delta^{18}O$ diagram for the NGB rocks and alteration end-members. Crosses represent whole-rock values dominated by amphiboles, circles are chloritized biotite. Field for altered modern oceanic crust is from [Stakes and O'Neil, 1982; Alt, 2012] and other sources. "Super" represents the average low-temperature submarine alteration end-member from Alt (2003). RA is computed metamorphic retrogression assemblage, which is generated by a mixture of chlorite and other micas with fractionation factors shown on the figure. Note that metamorphism and retrogression did not result in a significant shift in δD , and the trends can be explained by 1) initial alteration by a seawater having δD and $\delta^{18}O$ values comparable (or even slightly higher) than modern seawater, and 2) metamorphism and subsequent retrogression which did not involve any external low- δD meteoric or magmatic fluids. Isua field is from [Pope et al. 2012] for 3.8 Ga serpentinites from Greenland, interpreted to require lower δD seawater at 3.8 Ga.

minimal isotopic changes in rocks (on mm to cm scale). Perhaps paradoxically, one can argue that these crystalline metamorphic mineral assemblages lock the original surface oxygen into refractory phases, preventing them from further isotopic exchange and preserving the original protolithic composition throughout subsequent geologic and thermal history.

Hydrogen isotopes in Archean rocks were also used in prior studies to interpret early environments [Pope et al. 2012; Zakharov and Bindeman, 2019]. Ultra-low δ^{18} O rocks (-27.5‰) from Karelia also exhibit the world's lowest δD values measured so far (-235‰, with scatter to higher values) [Bindeman and Serebryakov, 2011]. The protolith of these rocks was flushed by ultra-low- δ^{18} O and thus ultra-low- δD glacial meltwaters, imprinting the water signature on the rocks. Thus, hydrogen isotopes may play a reinforcing role to O isotopes in order to trace the effects of water-rock interaction [Bowers and Taylor, 1985; Zakharov et al. 2021a].

Hydrogen isotopic values in the metamorphic NGB rocks need to be interpreted with caution and direction of metamorphic and other change discussed first. However, only few hydrogen isotope studies have been conducted on metamorphic rocks since the work of Valley (1986) showing that hydrogen isotopes are expected to be more strongly affected by metamorphism compared to oxygen as hydrogen is lost during devolatilization. First, during metamorphic devolatilization, which removed water heavier in δD , the original δD values of the hydrothermally-altered oceanic crust would shift to lighter isotopic composition (lower δD values), if the process were of Rayleigh-type (Valley, 1986) (**Fig. 7**). Second, fluxing by mantle-derived "magmatic" waters ($\delta D = -60$ to -80%) would also lower δD values of these rocks. Furthermore, if one argues that the Archean mantle was characterized by lower δD (and since

lost more H_2 than HD to the outer space, as is suggested by Pope et al. 2012), then fluxing by contemporaneous low- δD Archean mantle fluids would have had an even more dramatic effect on the NGB rocks. Finally, low-temperature chloritization by modern-day high-altitude local meteoric water (-150±20‰, waterisotopes.org) would generate a product that is still 60 to 90‰ lower in δD (Suzuoki and Epstein, 1976). NGB rocks were recently exposed by glacial scouring and samples were collected without any weathering features, so the effects of recent weathering are likely minimal.

Given that the high δD values of the NGB rocks are preserved, we suggest that the hydrogen isotopic composition, at least partially, originates from the original submarine hydrothermal alteration occurring at 4.3-3.8 Ga. Perhaps cumulative effects of metamorphic water cycle carried near-zero isotopic shift. For example, **Fig. 7** indicates that hydrothermal alteration of the basaltic protolith, and subsequent retrogression/chloritization of the assemblage at ~100-125°C is capable of explaining the data. The original δD values were redistributed and perhaps homogenized during metamorphism, but it appears that NGB rocks were not affected by a significant influx of external meteoric or magmatic fluids, all of which would have been lower in δD as we argued above.

Bounded to the debate about the age of the NGB metavolcanic rocks is the interpretation that the hydrothermal alteration processes affecting the Ujaraaluk rocks carrying low 142 Nd/ 144 Nd ratios is an obstacle to their geochronological interpretation (e.g. Caro et al., 2017). Roth et al. (2013) proposed that the variation in 142 Nd isotopic composition of the NGB rocks could be explained by partial isotope equilibration based on a fluid-mineral isotope exchange model. The new stable isotopic compositions obtained here can help better understand the post-magmatic processes affecting the NGB rocks in order to assess if the radiogenic isotopic evidence used for their geochronological interpretation was disturbed by hydrothermal fluids. **Figure 8** shows that the δ^{18} O values for the Ujaraaluk samples do not correlate with their μ^{142} Nd values, hydrothermal alteration processes that produced the high δ^{18} O values in most NGB samples and, the Ujaraaluk samples showing the largest 142 Nd anomalies (μ^{142} Nd = \sim -14) display δ^{18} O values between 7 and 7.5% while μ^{142} Nd = \sim -10 has δ^{18} O values 0f +11.5%. The lack of correlation between δ^{18} O and the μ^{142} Nd values implies that fluid-driven post-magmatic alteration is not responsible for the variation in 142 Nd observed in the NGB rocks, therefore strengthening

the argument that this variation in ¹⁴²Nd/¹⁴⁴Nd ratios holds a geochronological meaning (O'Neil et al., 2012; 2019).



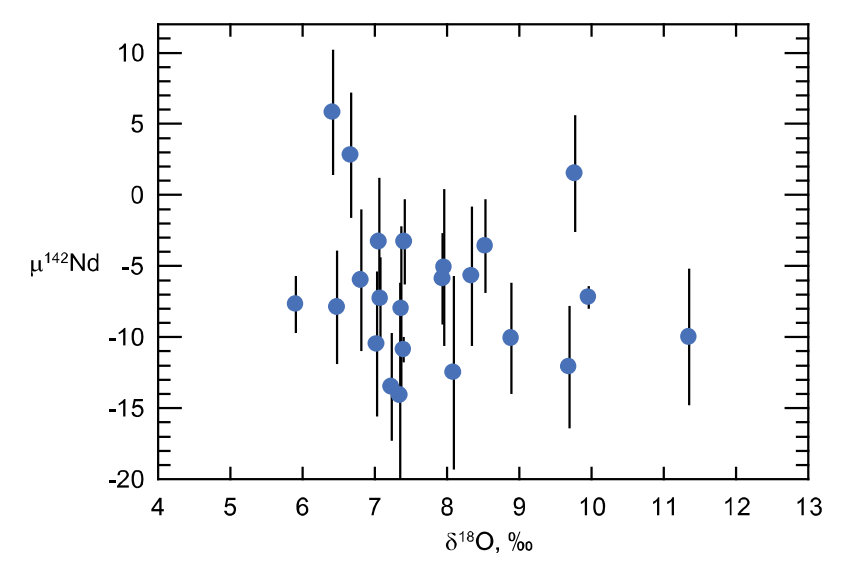


Fig. 8 μ^{142} Nd vs. δ^{18} O values for the NGB Ujaraaluk mafic metavolcanic rocks. No correlation between the δ^{18} O and μ^{142} Nd values suggests that the hydrothermal processes responsible for the variation in δ^{18} O values did not affect nor caused the variation in δ^{142} Nd isotopic composition. δ^{142} Nd isotopic data from O'Neil et al. (2012)

One of the main findings of this study is that the stable isotopic data that we obtained for one of the world's oldest, if not the oldest, section of oceanic crust require Hadean/Eoarchean oceans to be comparable to modern oceans with respect to triple oxygen and hydrogen isotopes (**Figs. 3-7**). Importantly, these values are also comparable to 2.4 Ga seawater inferred from beautifully preserved pillow lavas and their intrapillow hydrothermal fills, from the Vetreny Belt in Russia (Zakharov and Bindeman, 2019). These results depict a picture of constancy for seawater over the geological times despite evidence from sedimentary archives suggesting isotopically negative (down to δ^{18} O of -10 to -15‰) oceans showing a gradual increase of δ^{18} O with decreasing age [Shields and Veizer, 2002].

The triple oxygen relations (**Fig. 5 and 6**) allow reconstruction of hydrothermal temperature regime and seawater δ^{18} O values that may correspond to conditions in the early Archean/Hadean ambient ocean. As isotopically positive oceans were suggested by Johnson and Wing (2020), while discussion of isotopically negative oceans is a dominant theme of many studies involving sedimentary proxies [Shields and Veizer, 2002]. **Fig. 6** considers possibilities of seawater δ^{18} O values changing from -5 to +3‰. Oceans with -5‰ value would require lower temperature of water-rock interaction and lower water-rock ratios. Oceans with +3‰ would indicate much hotter interaction between rocks and water. Additionally, quartz would not fit on the quartz-water-equilibration curves, or under them. If diagenetic processes or secondary

alteration were to affect triple O isotope values of seawater-precipitated silica (e.g. Liljestrand et al. 2019; Hales et al. 2021), these processes would shift Δ^{17} O values under the curve, along a straight line connecting equilibrium values with waters (by analogy with a discordia line on a Concordia diagram for the U-Pb system). In this sense, -5‰ to 0 ‰ water remain as possible solutions, while +3‰ water would violate silica-water equilibrium.

We also note that the obtained silica-water equilibration temperatures are ~50-100°C higher than basalt-water equilibration temperatures. This may reflect that silica precipitation followed a disequilibrium path, requiring a rapid temperature drop causing silica to precipitate in open pore space (**Fig. 9**).

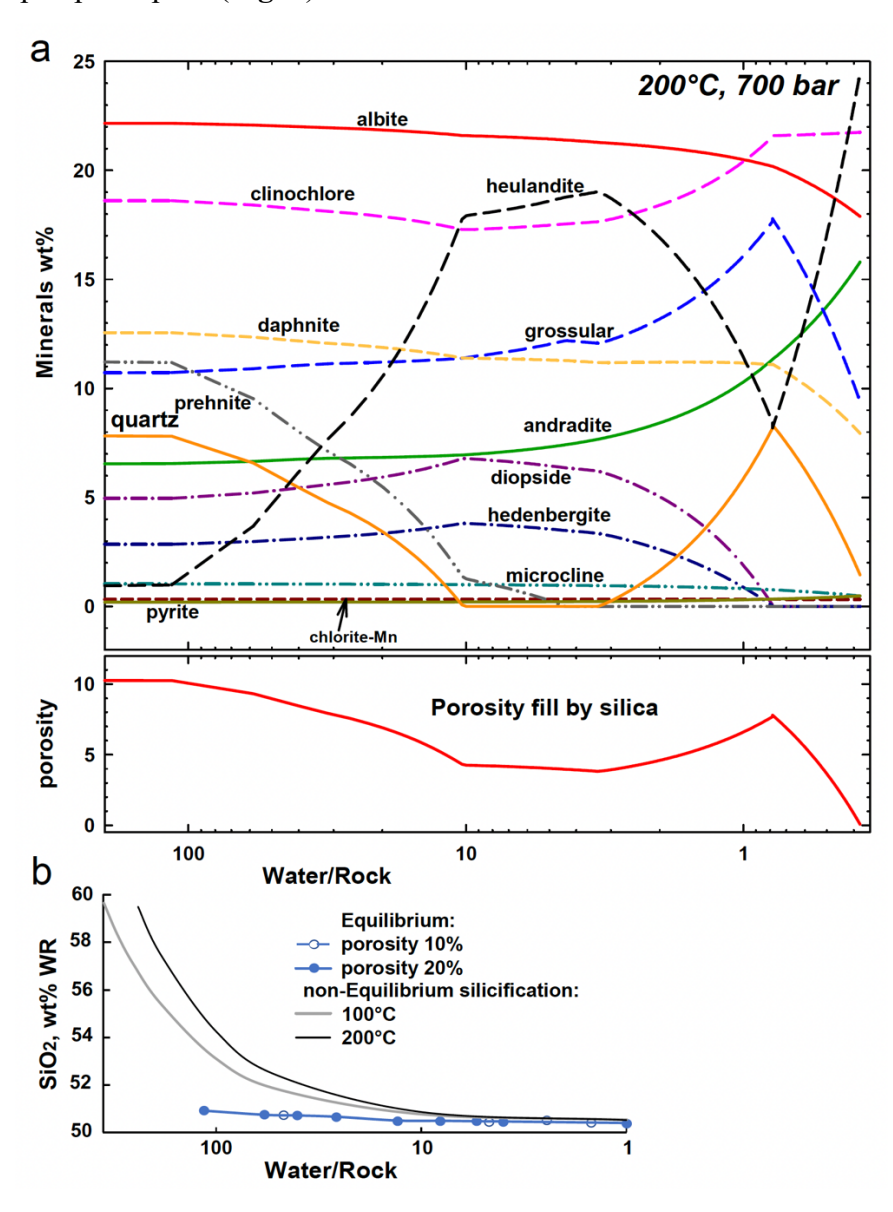


Fig. 9. Effects of silica-saturated seawater interaction with NGB basalts. (a) Output of equilibrium waterrock flushing computations showing mineralogical changes at different water-rock ratios and 10% porosity. Graph credit to James Palandri using the CHIM-XPT program Reed et al. [2010]. (b) compositional changes. Equilibrium flushing calculations without quartz precipitation resulting in insignificant change in bulk chemistry at any porosity. Simple precipitation of dissolved amorphous silica filling pore space is more efficient in increasing whole-rock SiO₂ content (orange curve labeled quartz in a).

Thus, our study suggests that Hadean/Eoarchean oceans, which contain abundant dissolved silica (in the absence of diatoms precipitation), contributed to the silicification of the NGB rocks. Such process is known in a wide variety of Eoarchean rocks highlighting the importance of syn-depositional hydrothermal activity for their origin (Hofmann and Bolhar, 2007; Zakharov et al. 2021).

More broadly, our study provides a reference point to the debate on the early tectonics and the geodynamic mechanisms that would balance high-temperature and low-temperature (subaerial and submarine weathering) geochemical processes that led to current global hydrosphere at around $\delta^{18}O = -0.75\%$. Low-temperature processes generate high- $\delta^{18}O$ lithospheric products and contribute low- $\delta^{18}O$ fluxes to the hydrosphere, while high-temperature alteration generates low- $\delta^{18}O$ products and high- $\delta^{18}O$ fluxes to the hydrosphere, to keep the $\delta^{18}O$ of the hydrosphere approximately constant [Holland, 1984; Muehlenbachs, 1998]. Given the boninitic affinities of some Ujaraaluk rocks [O'Neil et al. 2011; Turner et al., 2014], the formation of the NGB could have involved subduction-initiation type environments, at least short-lived and perhaps locally [O'Neil et al. 2016].

Alternatively, in the absence of modern-style plate tectonics and subduction (return isotopic flux to the mantle), an early Earth dominated by plume tectonics with hotter mantle [Bedard, 2018; Stern et al. 2018]. With little subaerially exposed crust available for weathering (e.g. [Bindeman et al. 2018]), our results of relatively constant $\delta^{18}O$ of seawater would then call for more predominant role of low-temperature submarine hydrothermal alteration and submarine weathering [Coogan and Gillis, 2018], as well as precipitation of silica from seawater, to counterbalance the high-temperature ocean-lithosphere interaction (Hoffman et al. 1986). As the high-temperature (lower- $\delta^{18}O$) domain typically found in sections of oceanic crust appears to be missing from the NGB, one can speculate that due to higher geothermal gradient, and or clogging of hydrologic pathways by secondary silica, as documented here, seawater was mostly

circulating in the shallow portion of the oceanic crust. Thus, submarine weathering appears to

have played the dominant role in the early Earth oceanic crustal history.

Acknowledgements

INB thanks NSF grant EAR 1833420, Jim Palandri for analytical help. Fieldwork during which JO collected the NGB samples was facilitated by the Pituvik Landholding Corporation of Inukjuak and funded by the National Science and Engineering Research Council of Canada.

Reviews by three anonymous reviewers and editorial comments by Laurence Coogan are greatly

Reviews by three anonymous reviewers and editorial comments by Laurence Coogan are greatly acknowledged.

References

- Alt, J.C. and Teagle, D.A.H., 2003. Hydrothermal alteration of the upper oceanic crust formed at a fast-spreading ridge: Mineral, chemical, and isotopic evidence from ODP Site 801. Chemical Geology 201, 191-211.
- Alt, J.C. and Teagle, D.A.H., 2000. Ophiolites and Oceanic Crust: New insights from field studies and the Ocean Drilling Program. Geological Society of America Special Paper 349, 273-282.
- Alt, J.C., 2003. Stable isotopic composition of upper oceanic crust formed at a fast-Spreading ridge, ODP Site 801, Geochem. Geophys. Geosyst., 4(5), 8908,doi:10.1029/2002GC000400
- Alt, J.C., Garrido, C.J., Shanks W.C. III, Turchyn, A. et al. 2012. Recycling of water, carbon, and sulfur during subduction of serpentinites: A stable isotope study of Cerro del Almirez, Spain. Earth Planet. Sci. Lett. 327–328, 50-60.
- Andrée, L., Abraham, K., Hofmann, A., Monin, L., Kleinhanns, I.C., Foley, S., 2019. Early Continental crust generated by reworking of basalts variably silicified by seawater. Nature Geoscience 12, 769–773.
- Bédard, J.H., 2018. Stagnant lids and mantle overturns: Implications for Archaean tectonics, magma genesis, crustal growth, mantle evolution, and the start of plate tectonics. Geoscience Frontiers 9, 19-49.
- Bindeman, I.N., 2021. Triple oxygen isotopes in evolving continental crust, granites, and clastic sediments. Reviews in Mineralogy and Geochemistry 86, 8), 241-290
- Bindeman, I.N., Zakharov, D., Palandri, J., Greber, N.D., Retallack, G.J., Hoffman, A., Dauphas, N., Lackey, J.S., Bekker, A., 2018. Rapid growth of subaerial crust and the onset of a modern hydrologic cycle at 2.5 Ga. Nature 557 (7706), 545-548
- Bindeman, I.N., Serebryakov, N.S., 2011. Geology, Petrology and O and H isotope geochemistry of remarkably ¹⁸O-depleted Paleoproterozoic rocks of the Belomorian Belt, Karelia, Russia, attributed to global glaciation 2.4Ga. Earth Planet. Sci. Lett. 306, 163-174.
- Bowers, T.S., Taylor, H.P., 1985. An integrated chemical and isotope model of the origin of midocean ridge hot spring systems. J. Geophys. Res. 90, 12583–12606.
- Caro, G., Morino, P., Mojzsis, S. J., Cates, N. L., & Bleeker, W., 2017. Sluggish Hadean geodynamics: Evidence from coupled ^{146,147}Sm–^{142,143}Nd systematics in Eoarchean supracrustal rocks of the Inukjuak domain, Québec). Earth Planet. Sci. Lett. 457, 23–37.
- Cates, N.L., Ziegler, K., Schmitt, A.K. & Mojzsis, S.J., 2013. Reduced, reused and recycled:
 detrital zircons define a maximum age for the Eoarchean, (ca. 3750–3780 Ma)
 Nuvvuagittuq supracrustal belt, Québec, Canada). Earth Planet. Sci. Lett. 362, 283–293.
- Coogan, L.A. and Gillis, K.M. 2018. Low-temperature alteration of the seafloor: Impact on ocean chemistry. Annual Review of Earth and Planetary Sciences 46, 21-45.

658 Cr aig, H., 1966. Isotopic composition and origin of the Red Sea and

665

666 667

668

669

670

671

672

673 674

675

676

677 678

679

680

681

682

683 684

685

686

687

691

692

- Coulthard, D.A., Reagan, M.K., Shimizu, K., Bindeman, I.N., Brounce, M., Almeev, R.R. et al. 2021. Magma source evolution following subduction initiation: Evidence from the element concentrations, stable isotope ratios, and water contents of volcanic glasses from the Bonin forearc, IODP expedition 352). Geochemistry, Geophysics, Geosystems, 22, e2020GC009054. https://doi.org/10.1029/2020GC009054. David, J., Godin, L., Stevenson, R., O'Neil, J., and Francis, D., 2009, U-Pb ages, 3.8-2.7 Ga, and
 - David, J., Godin, L., Stevenson, R., O'Neil, J., and Francis, D., 2009. U-Pb ages, 3.8-2.7 Ga. and Nd isotope data from the newly identified Eoarchean Nuvvuagittuq supracrustal belt, Superior Craton, Canada. Geological Society of America Bulletin, 121, 150-163.
 - DePaolo, D.J., 2006. Isotopic effects in fracture-dominated reactive fluid–rock systems. Geochim. Cosmochim. Acta 70, 1077–1096.
 - Dixon, J.E., Bindeman, I.N., Kingsley, R.H., Simons, K.K., Le Roux, P.J., Hajewski, T.R. et al. 2017. Light stable isotopic compositions of enriched mantle sources: Resolving the dehydration paradox. Geochemistry, Geophysics, Geosystems 18, 3801–3839. https://doi.org/10.1002/2016GC006743
 - Dodd, M., Papineau, D., Grenne, T. et al., 2017. Evidence for early life in Earth's oldest hydrothermal vent precipitates. Nature 543, 60–64.
 - Eiler, J.M., 2001. Oxygen isotope variations of basaltic lavas and upper mantle rocks. Rev. Mineral. Geochem. 43, 319–364
 - Farahat, N. X., Archer, D. and Abbot, D. S., 2017. Validation of the BASALT model for simulating off-axis hydrothermal circulation in oceanic crust, J. Geophys. Res. Solid Earth, 122, 5871–5889, doi:10.1002/2016JB013758
 - Friedman, I., and O'Neil, J.R. 1977. Compilation of stable isotope fractionation factors of geochemical interest; U.S. Geol. Surv. Prof. Paper 440-KK.
 - Gregory, R.T., Taylor, H.P., 1981. An oxygen isotope profile in a section of Cretaceous oceanic crust, Samail ophiolite, Oman: evidence for δ¹⁸O buffering of the oceans by deep, 5 km. seawater-hydrothermal circulation at mid-ocean ridges. J. Geophys. Res. Solid Earth 86, 2737–2755.
 - Johnson, B.W., Wing, B.A., 2020. Limited Archaean continental emergence reflected in an early Archaean 18-O-enriched ocean. Nature Geoscience 13, 243-248
- Harrison, T.M. (2020) Hadean Earth. Springer-Nature, 291 p.
- Herwartz, D., 2021. Triple oxygen isotope variations in Earth's crust. Rev. Mineral. Geochem. 86, 291–322.
 - Hofmann, A. and Bolhar, R., 2007. Carbonaceous cherts in the Barberton Greenstone Belt and their significance for the study of early life in the Archean Record. Astrobiology 7, 355-388 http://doi.org/10.1089/ast.2005.0288
- Hoffman, S., Wilson, M. & Stakes, D. 1986. Inferred oxygen isotope profile of Archaean oceanic
 crust, Onverwacht Group, South Africa. Nature 321, 55–58.
 https://doi.org/10.1038/321055a0
- Holland, H.D., 1984. The chemical evolution of the atmosphere and oceans. Princeton University Press 559p
- Kanzaki, Y., 2020a. Interpretation of oxygen isotopes in Phanerozoic ophiolites and sedimentary rocks. Geochem. Geophys. Geosyst. 21, e2020GC009000.
- Kanzaki, Y., 2020b. Quantifying the buffering of oceanic oxygen isotopes at ancient midocean ridges. Solid Earth 11, 1475–1488.
- Korenaga, J., Planavsky, N. J., and Evans, D.A.D. 2017. Archean geodynamics and the thermal evolution of Earth. Phil. Trans. R. Soc. A, 375, 20150393.
- Kasting, J.F., Howard, M. T., Wallmann, K., Veizer J., Shields, G. and Jaffrés, J., 2006.
- Paleoclimates, ocean depth, and the oxygen isotopic composition of seawater. Earth Planet. Sci. Lett. 252, 82–93.
- Knauth, L.P., Lowe, D.R., 2003. High Archean climatic temperature inferred from oxygen

- isotope geochemistry of cherts in the 35 Ga Swaziland Supergroup, South Africa. Bull Geol. Soc. Am. 115, 566-580.
- Liljestrand, F. L., Knoll A. H., Tosca N. J., Cohen P. A., Macdonald F. A., Peng Y. and
 Johnson D. T., 2020. The triple oxygen isotope composition of Precambrian chert. Earth
 Planet. Sci. Lett. 537, 116167
- Miller, M.F., Pack, A., Bindeman, I.N., Greenwood, R.C., 2020. Standardizing the reporting of Δ'^{17} O data from high precision oxygen triple-isotope ratio measurements of silicate rocks and minerals. Chem. Geol. 532:119332,
- 717 Mloszewska, A. M., Mojzsis, S.J., et al., 2013. Chemical sedimentary protoliths in the ~3.75Ga 718 Nuvvuagittuq supracrustal belt, Québec, Canada). Gondwana Res. 23, 574–594
- Muehlenbachs, K., 1998. The oxygen isotopic composition of the oceans, sediments and the seafloor. Chem. Geol. 145, 263–273
- Muehlenbachs, K., Clayton, R.N., 1976. Oxygen isotope composition of the oceanic crust and its bearing on seawater. J. Geophys. Res. 81, 4365–4369.
- O'Neil, J., Carlson, R. W., Francis, D. & Stevenson, R. K., 2008. Neodymium-142 evidence for Hadean mafic crust. Science 321, 1828–1831.
- O'Neil, J., Carlson, R. W., Paquette, J.-L. & Francis, D., 2012. Formation age and metamorphic history of the Nuvvuagittuq greenstone belt. Precamb. Res. 220–221, 23–44.
- O'Neil, J., Francis, D. & Carlson, R. W., 2011. Implications of the Nuvvuagittuq greenstone belt for the formation of Earth's early crust. J. Petrol. 52, 985–1009.
 - O'Neil, J., Carlson, R.W., Papineau, D., Levine, Y.E., Francis, D., 2019. Chapter 16: The Nuvvuagittuq Greenstone Belt: A Glimpse of Earth's Earliest Crust in Earth's Oldest Rocks, Second Edition), 349-374
- Papineau, D., deGrigorio, B.T. et al., 2001. Young poorly crystalline graphite in the >3.8-Gyr-old Nuvvuagittuq banded iron formation. 4, 376-379.

731

- Pope, E.C., Bird, D.K., Rosing, M.T., 2012. Isotope composition and volume of Earth's early oceans. PNAS 109, 12. 4371-4376.
- Qi, H., Coplen, T. B., Gehre, M., Vennemann, T. W., Brand, W. A., Geilmann, H., Olack, G.,
 Bindeman, I. N., Palandri, J., Huang, L. and Longstaffe, F. J., 2017. New biotite and muscovite isotopic reference materials, USGS57 and USGS58, for δ2H measurements A replacement for NBS 30. Chem. Geol. 467, 89–99.
- Qi, H., Gröning, M., Coplen, T. B., Buck, B., Mroczkowski, S. J., Brand, W. A., Geilmann, H. and
 Gehre, M., 2010. Novel silver-tubing method for quantitative introduction of water into high temperature conversion systems for stable hydrogen and oxygen isotopic measurements. Rapid
 Commun. Mass Spectrom. 24, 1821–1827.
- Perry, E.C. Jr.,1967. The oxygen isotope chemistry of ancient cherts. Earth Planet. Sci. Lett. 3, 62–66.
- Rumble, D., Yui, T.F., 1998. The Qinglongshan oxygen and hydrogen isotope anomaly near Donghai in Jiangsu Province, China. Geochim. Cosmochim. Acta 62, 3307–3321.
- Reed, M.H., Spycher, N.F., J. Palandri, J., 2010. Users Guide for CHIM-XPT: A Program for Computing Reaction Processes in Aquous-Mineral Gas Systems and MINITAB Guide. University of Oregon, Eugene, OR, 2010)
- Roth, A.S.G., Bourdon, B., Mojzsis, S.J., Touboul, M., Sprung, P., Guitreau, M., & Blichert-Toft, J., 2013. Inherited ¹⁴²Nd anomalies in Eoarchean protoliths. Earth Planet. Sci. Lett. 361, 50–57.
- Savin, S., Lee, M.L., 1988. Isotopic studies of hydrous phyllosilicates. In Hydrous Phyllosilicates.
 In: Bailey, S.W., Ed., Hydrous Phyllosilicates, Reviews in Mineralogy 19, 189-223
- 756 Sengupta, S., Pack A., 2018. Triple oxygen isotope mass balance for the Earth's oceans with

757 application to Archean cherts. Chem. Geol. 495, 18-26

- Shields, G., and Veizer, J., 2002. Precambrian marine carbonate isotope database: Version 1.1. Geochemistry, Geophysics, Geosystems 3, 6), 1-12.
 - Stern, R.J., Gerya, T., Tackley, P.J., 2018. Stagnant lid tectonics: Perspectives from silicate planets, dwarf planets, large moons, and large asteroids. Geoscience Frontiers 9, 103-119 Sharp, Z.D., 2017. Stable Isotope Geochemistry, 2nd edition, https://doi.org/10.25844/h9q1-0p82
 - Sharp, Z.D., Gibbons, J.A., Maltsev, O., Atudorej, V., Pack, A, Sengupta, S., Shock, E.L., Knauth, L.P., 2016. A calibration of the triple-isotope fractionation in the SiO2–H2O system and applications to natural samples. Geochim Cosmochim Acta 186, 105–119
 - Stakes, D.S. and O'Neil, J.R., 1982. Mineralogy and stable isotope geochemistry of hydrothermally altered oceanic rocks. Earth Planet Sci Lett 57, 285-304.
 - Schauble, E., Young, E., 2021. Mass dependence of equilibrium oxygen isotope fractionation in carbonate, nitrate, oxide, perchlorate, phosphate, silicate, and sulfate minerals. Rev. Mineral. Geochem. 86, 137–178.
 - Tartèse, R., Chaussidon, M., Gurenko, A., Delarue, F. and Robert, F., 2017. Warm Archean oceans reconstructed from oxygen isotope composition of early-life remnants. Geochem. Persp. Lett. 3, 55–65.
- Turner, S., Rushmer, T., Reagan, M. & Moyen, J.-F., 2014. Heading down early on? Start of subduction on Earth. Geology 42, 139–142.
- Valley, J.W., 1986. Stable isotope geochemistry of metamorphic rocks: Reviews in
 Mineralogy 16, 445–489.
- Valley, J.W., Kitchen, N., Kohn, M.J., Niendorf, C.R., and Spicuzza, M.J.,1995. UWG-2, a garnet standard for oxygen isotope ratio: Strategies for high precision and accuracy with laser heating: Geochim. Cosmochim. Acta 59, 5223–5231.
- Valley, J.W., Peck, W.H., King, E.M., Wilde S.M. 2002. A cool early Earth. Geology 30, 351-354.
- Wostbrock, J.A.G., Sharp, Z.D., 2021. Triple Oxygen Isotopes in Silica–Water and Carbonate–Water Systems. Rev. Mineral. Geochem. 86, 367-400.
- Zakharov, D.O., Lundstrom, C.C., Laurent, O., Reed, M.H., Bindeman, I.N., 2021. Influence of high marine Ca/SO₄ ratio on alteration of submarine basalts at 2.41 Ga documented by triple O and Sr isotopes of epidote. Prec. Res. 358, 106164
 - Zakharov, D.O., Marin-Carbonne, J., Alleon, J., Bindeman, I.N., 2021. Triple Oxygen Isotope Trend Recorded by Precambrian Cherts: A Perspective from combined bulk and in situ Secondary Ion Probe Measurements. Rev. Mineral. Geochem. 86, 323-366.
 - Zakharov, D.O., Bindeman, I.N., 2019. Triple oxygen and hydrogen isotopic study of hydrothermally altered rocks from the 2.43–2.41 Ga Vetreny belt, Russia: An insight into the early Paleoproterozoic seawater. Geochim. Cosmochim. Acta 248, 185-209
 - Zakharov, D.O., Tanaka, R., Butterfield, D.A., Nakamura, E., 2021. A New insight into seawater-basalt exchange reactions based on combined δ¹⁸O-Δ'¹⁷O-⁸⁷Sr/⁸⁶Sr values of hydrothermal fluids from the Axial Seamount Volcano, Pacific Ocean. Frontiers in Earth Science 9, 691699
 - Zhao, Z.-F., Zheng, Y.F., 2003. Calculation of oxygen isotope fractionation in magmatic rocks. Chem. Geol. 193, 59-80.

Data and materials availability: All data are available in the main text or the supplementary materials.

807 **Figure Captions** 808 809 Fig. 1 Simplified geological map of the Nuvvuagittug greenstone belt from O'Neil et al. [2011]. 810 Locations for the metabasaltic samples analyzed for this study are shown, with color and size of the symbols corresponding to measured $\delta^{18}O_{rock}$ values. 811 812 813 Fig. 2 Field photograph of preserved deformed pillow lavas in the Ujaraaluk unit, with differential 814 erosion highlighting the selvages of the single pillows. 815 816 Fig. 3 a) Histogram of the δ^{18} O and v δ D values (inset) in the different rock types of the Nuvvuagittuq greenstone belt and **b)** Al₂O₃/TiO₂ ratios vs. δ¹⁸O values for different compositional groups of Uiaraaluk 817 metabasalts. Data are presented in Table 1. MORB δ^{18} O and v δ D values are from Gregory and Taylor 818 819 (1981) and Dixon et al. (2017). 820 Fig. 4 δ^{18} O vs SiO₂ diagrams for the NGB Ujalaaluk rocks (blue symbols), a) full SiO₂ range of all 821 822 analyzed lithologies, b) zoomed in range (see Table 1 for data) focusing on the Ujaraaluk samples. 823 Modern boninite suite from [Coulthard et al. 2020] is shown for comparison, as some NGB rocks are 824 analogous to boninites [O'Neil et al., 2011; Turner et al. 2014]. Igneous differentiation of MORB basalts 825 would result in negligible increase of δ^{18} O values (by 0.1-0.2%; [Eiler, 2001]) as is also exemplified by 826 the boninite suite. Low temperature ($<150^{\circ}$ C) alteration can account for the range and increase in δ^{18} O 827 values observed in the NGB rocks, while addition of chemogenically-precipitated SiO₂ can also explain 828 the positive correlation with SiO₂. Ca-depleted are cordierite-anthophyllite rocks, are interpreted to have 829 lost most Ca due to hydrothermal alteration [O'Neil et al., 2019]. 830 Fig. 5 Triple oxygen isotopes for the studied rocks compared to the Δ^{17} O- δ^{18} O Qz-water fractionation 831 832 curve [from Sharp et al., 2016] emanating from the modern ocean water, and basalt-seawater lines. 833 computed in this work. Notice that the NGB rocks plot between mixing lines connecting mantle-derived 834 rocks and seawater-equilibrated hydrothermally-altered component(s) at temperature of alteration 835 between >45°C and <150°C (yellow triangular field). Seafloor and subaerial weathering occurring at low temperature would lead to much lower Δ^{17} O values and is not supported by the data. Concurrent 836 837 silicification trends produced by silica precipitated from seawater are shown by orange arrows extending 838 from the vellow triangular field.

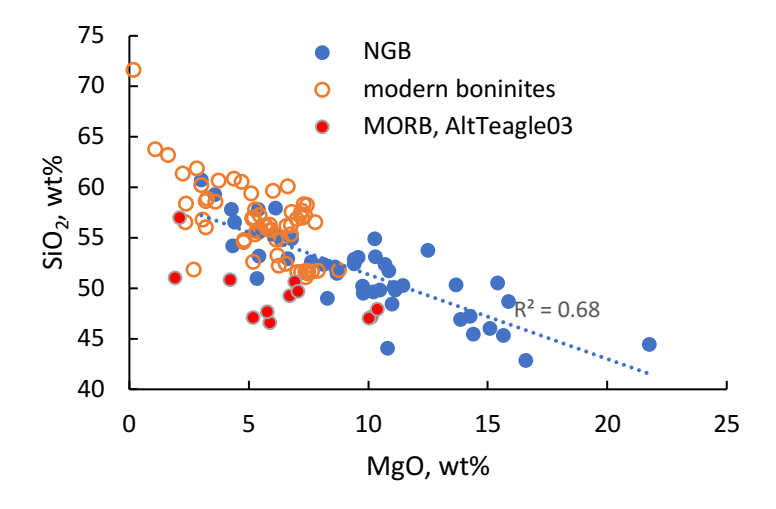
Fig. 6. Triple oxygen isotopic data (same data as in Fig. 5) but assuming different δ^{18} O values of 840 seawater, ranging from -5 to +3\%. Change in δ^{18} O is accompanied by a change in Δ^{17} O along a blue line 841 with a slope of 0.521 [Bindeman, 2021]. Assuming a water value of -5% would result in ~20° to 150°C 842 843 temperature of water-rock interaction and silicification, as well as lower water/rock ratios (illustrated on green inset). Assuming seawater with a $\delta^{18}O$ value of +3% would result in higher temperatures of 844 845 interaction (~80° to 400°C) and greater water-rock ratios for basalt-water interaction; in addition, quartz 846 samples would plot outside of realistic quartz-water equilibration curves. 847 **Fig. 7** Hydrogen- H_2O and $\delta^{18}O$ correlation for NGB rock suite. 848 849 a) δD – H₂O diagram comparing the NGB rocks and modern (Cenozoic) hydrothermally altered seafloor 850 products [Bowers and Taylor, 1985; Alt, 2003; Stakes and O'Neil, 1982; Alt and Teagle, 2003]. \deltaD 851 values of mantle and modern boninites are shown for comparison. Various isotopic shift trends from 852 known processes are represented with arrows [Valley, 1986; Bindeman and Serebryakov, 2010]. Notice 853 that an increase in water content in the NGB rocks is not accompanied by a decrease in δD , suggesting 854 that it was caused by a fluid comparable to seawater during hydrothermal or metamorphic processes. 855 There is no difference in δD values between coexisting anthophyllite, biotite and whole-rock, within the 856 same rock samples (Table 1). 857 b) δD vs $\delta^{18}O$ diagram for the NGB rocks and alteration end-members. Crosses represent whole-rock 858 values dominated by amphiboles, circles are chloritized biotite. Field for altered modern oceanic crust is 859 from [Stakes and O'Neil, 1982; Alt, 2012] and other sources. "Super" represents the average low-860 temperature submarine alteration end-member from Alt (2003). RA is computed metamorphic 861 retrogression assemblage, which is generated by a mixture of chlorite and other micas with fractionation 862 factors shown on the figure. Note that metamorphism and retrogression did not result in a significant shift 863 in δD , and the trends can be explained by 1) initial alteration by a seawater having δD and $\delta^{18}O$ values 864 comparable (or even slightly higher) than modern seawater, and 2) metamorphism and subsequent 865 retrogression which did not involve any external low-δD meteoric or magmatic fluids. Isua field is from 866 [Pope et al. 2012] for 3.8 Ga serpentinites from Greenland, interpreted to require lower δD seawater at 3.8 867 Ga. 868 Fig. 8 μ^{142} Nd vs. δ^{18} O values for the NGB Ujaraaluk metavolcanic rocks. No correlation between the 869 870 δ^{18} O and μ^{142} Nd values suggests that the hydrothermal processes responsible for the variation in δ^{18} O values did not affect nor caused variation in ¹⁴²Nd isotopic composition. ¹⁴²Nd isotopic data from O'Neil 871 872 et al. (2012).

Fig. 9. Effects of silica-saturated seawater interaction with NGB basalts. (a) Output of equilibrium waterrock flushing computations showing mineralogical changes at different water-rock ratios and 10% porosity. Graph credit to James Palandri using the CHIM-XPT program Reed et al. [2010]. (b) compositional changes. Equilibrium flushing calculations without quartz precipitation resulting in insignificant change in bulk chemistry at any porosity. Simple precipitation of dissolved amorphous silica filling pore space is more efficient in increasing whole-rock SiO₂ content (orange curve labeled quartz in a).

SUPPLEMENTARY MATERIAL

Supplementary S1 Supplementary Table S1 with stable isotopic data and previously published compositional data in Excel form







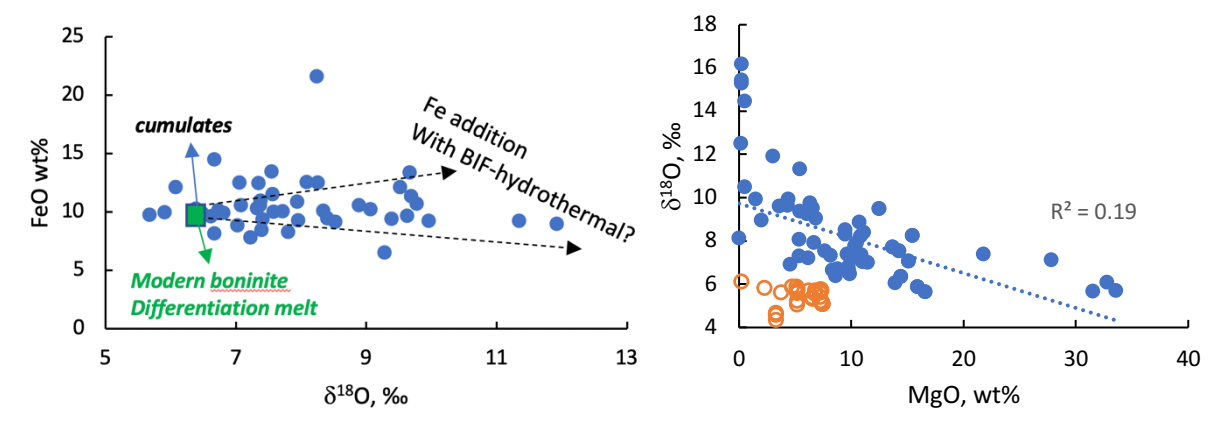


Fig. S1 Compositional ranges in NGB suite display features of the original igneous protolith and masking effects of both igneous fractionation and hydrothermal alteration. In particular, ${\rm SiO_2}$ correlates with MgO along a straight line indicative of mixing rather than differentiation, however modern boninites exhibit comparable correlation in the lower part of the MgO spectrum. High-MgO samples can represent cumulates (O'Neil et al. 2011). There are no statistically significant correlations of $\delta^{18}{\rm O}$ or ${\rm SiO_2}$ with any other major or trace elements, or indices of alteration such as Alk/Al or CIA, and water concentration suggesting that several processes are in operation including igneous differentiation of diverse magma types and various extent of hydrothermal alteration, which complicated these trends.

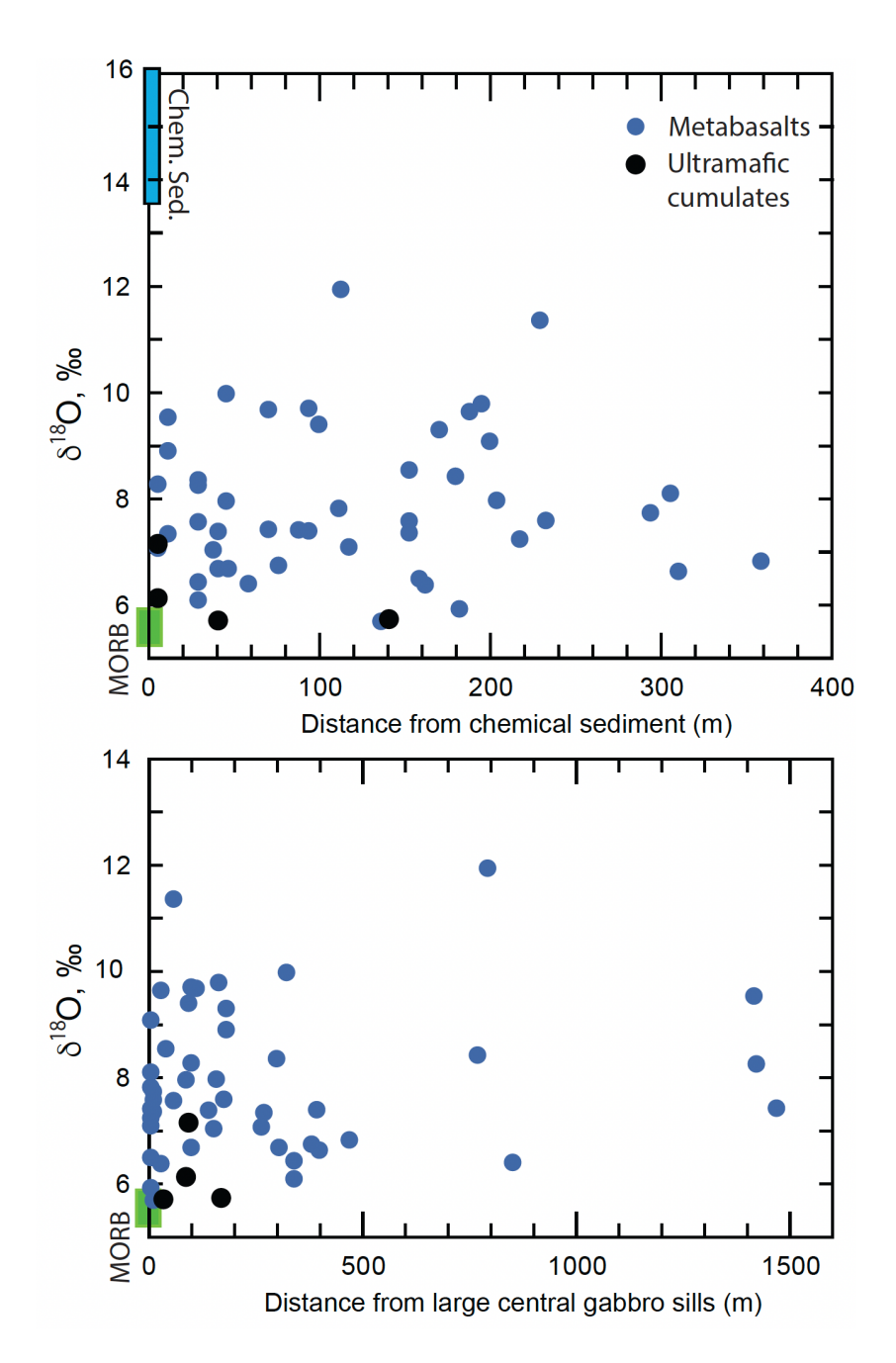


Fig. S2. Lack of correlation between $\delta^{18}O$ and distance from silica formation and large central gabbro body suggesting that hydrothermal alteration are independent of these.